D－1　渤海・東シナ海における河川経由の環境負荷が海洋生態系に与える影響評価手法に関する研究

（3）生態系モデルによる環境負荷の影響評価手法に関する総合的研究

②　渤海・東シナ海の海洋環境データベース化と流動モデル開発に関する国際交流研究

研究代表者　国立環境研究所　水土壌圏環境部　部長　　渡辺正孝

エコフロンティアフェロー

The First Institute of Oceanography, SOA (China)	Qiao Fangli	(1996)
Nanjing Hydrolic Research Institute (China)	Dou Xiping	(1997)
The Second Institute of Oceanography, SOA (China)	PAN Jianming	(1998)

平成８年度～１０年度合計予算額　6,011 千円

（平成１０年度予算額　2,003 千円）

[要旨]

渤海・東シナ海の流動は黒潮、潮汐、河川からの淡水流入、風・気象条件により影響を受け抜雑な流況を呈する。過去に多くの数値モデルによる解析が試みられたが、十分な検証に基づく解析は少なかった。本研究では Blumberg and Mellor により開発された Princeton Ocean Model（POM）を用いて渤海・東シナ海の潮汐流についての解析を行った。計算領域は 177°E～131°E、24°N～41.5°N で、グリッドは 0.25°×0.25°、鉛直方向に 11 層とした。Smagorinsky の水平渦拡散係数は 0.1、Δt=45 秒とした。境界条件として $(K_1 + O_1)$と(M_2)を与え、さらに黒潮の流れに起因する平均的水位を与えた。黒潮による平均流量は 30Sv.とした。100 日シミュレーションの計算結果は、沿岸潮汐観測点 81 カ所での実測データによる調和定数の振幅、位相について比紋を行い良好な一致を得た。また計算された黒潮は、過去の観測結果の平均値とよく合致した。対馬海峡においては九州側で東シナ海から日本海に入る流れが、韓国側では日本海から東シナ海への流れが計算された。台湾暖流が東シナ海の南部の流況を支配していることが計算結果から再現された。

長江の流れに含まれる大量の流砂は大部分が河口域に沈降する。しかし潮流と風波の影響によって、流砂は再浮上し移送過程を通じて複雑な堆積形状をもたらす。本研究では長江河口域での流砂分布及び堆積した海底形状について、長江からの流砂供給、淡水供給を境界条件として水平 2 次元数値モデルを用いた解析を行った。モデル計算結果は、潮流および濁度の 1 ヶ月間連続観測値を用いて検証し、よい再現性を確認した。

1950 年初期から 1980 年初期にかけての中国における有機塩素系農薬使用により長江河口域での海洋環境は汚染されていたと考えられる。しかし 1980 年代初期において DDT、BHC 等の使用禁止後、それらの濃度は減少し、堆積物中の DDT、BHC 濃度はそれぞれ 0.25～0.31ng/g 及び 0.35～0.47ng/g 程度にまで減少した。これらの値は世界の他の河口域での値と比較しても特に高い値とは言えない。これは長江上流域からの流砂量が非常に多いこと、長江河口域での堆積速度が高いことに起因する。堆積物コアーは DDT、BHC 等汚染物質の過去の汚染を記録しているが、コアーの深い(年代の古い)部分では DDT、BHC とも高い濃度を示すが、コアーの浅い(年

代の新しい)部分では低い濃度を示す。このことから長江河口域においては DDT、BHC 負荷は近年減少してきていることが示唆された。

[キーワード]　東シナ海、渤海、長江河口域、潮汐流、流砂、数値モデル、堆積物

D-1.3.2 Database of Marine Environment and Circulation Simulation in East China Sea (Final Report)

Contact Person Masataka Watanabe
Director,
Division of Water and Soil Environment
National Institute for Environmental Studies
Environment Agency
16-2 Onogawa, Tsukuba, Ibaraki 305, Japan
Tel.: 81-298-50-2338, Fax: 81-298-50-2576
E-mail: masawata@nies.go.jp

Total Budget for FY1996-FY1998 **6,011,000 Yen (FY1998; 2,003,000 Yen)**

Abstract

Based on a three-dimensional primitive-equation dynamic numerical model, the general circulation of the East China Sea and the Yellow Sea is studied with a 0.25 x 0.25 horizontal grid and a realistic bottom topography. We consider the tide current and Kuroshio simultaneously. The model tide harmonic constants agree very well with the 81 coastline stations' observations in this area. The path of the Kuroshio agrees with long-term observations; a branch of the Kuroshio enters the East China Sea and reaches nearly 29N, and thus controls a large part of the East China Sea. A branch of the Kuroshio goes northward and forms the Tsushima warn current.

In order to know the silt quantity of the navigation channel in Changjiang estuary, a horizontal 2-D numerical model of both suspended and bed load transport in the area is established. The suspended and bed load transport equations and sediment transport capacity formulas under the action of tidal currents and wind waves have been used. It applies an automatically generated boundary-fitted grid with orthogonal curvilinear coordinates. The verification of calculation shows the sediment concentration and the deformation of sea bed can be successfully simulated.

The usage of organochlorine pesticides during early 1950s to early 1980s had polluted the marine environment of the Changjiang Estuary. But after banned using, DDT and BHC content in newest sediments decreased rapidly to 0.25~0.31ng/g and 0.35~0.47ng/g respectively. Compared with data before 1980, DDT and BHC content in sediments of the Changjiang Estuary reached relative lower level. due to dilution of a large amount bedload from upper Changjiang River and high sedimentary rate in the Changjiang Estuary.

Key Words East China Sea, Changjiang Estuary, Numerical Model, Tidal Current, Silt, Sediment

1. General Circulation Simulation of the East China Sea and the Yellow Sea

1.1. Introduction

The hydrodynamic characteristics of the East China Sea and the Yellow Sea is mainly affected by the Kuroshio, tide forcing, fresh water input by large rivers, water exchange through the Tsushima Strait, water density distribution and meteorology conditions. For tide numerical simulation, there are more than 20 papers, most study areas are small, with the exception of Sheng Y. J. (1980). Choi B H (1980,1984), Shen Y. J. and Ye Anle (1985), Fang G. (1986) and Zhao B. et al (1994). They still simplify the numerical models by omitting the nonlinear term. Choi set the boundary at the shelf edge of the East China Sea to avoid instability. Zhao et al (1994) and Fang (1986)'s model results are more reliable.

Many works only concern the Kuroshio. Chen C. et al (1992), Kaneko A. et al (1992,1993) and Kawabe M. based their work on data analysis. Qiu B. et al (1990) numerically studied the formation of the Kuroshio counter current and the Kuroshio branch currents. Kubota M. et al (1995) analyzed the mechanism of the seasonal transport variation in the Tokara Strait. Takahashi S. et al (1995 a, b) simulated the circulation in the Yellow Sea during summer and winter with simplified topography. The mechanism of different circulation patterns is explained. Kagimoto T. and Yamagata T. (1997) use the Princeton Ocean Model (hereafter called POM) to simulate the seasonal variation of the Kuroshio transport. The model results are very consistent to observations. This is a good way to avoid lateral boundary conditions, but it requires much CPU time and the horizontal resolution can not practically be high.

In the present study, we ran a high resolution POM to minic the general circulation in the East China Sea and the Yellow Sea. Although many factors influence the circulation, as the first step, we considered the Kuroshio and tide current simultaneously. The modeled basic pattern is consistent to observations, and the model results of tide harmonic constants are very accurate.

1.2. Numerical model and boundary conditions

The numerical model adopted in the present study is POM with primitive equations and Boussinesq approximations. It has been successfully used in many regions all over the world. Details of the POM and its development are given in Mellor et al (1982,1985 and 1994) and Blumberg et al (1983,1987a and 1987b) and therefore will not be repeated here. The model was used in the South China Sea to validate tide and typhoon induced currents (Qiao F. L. et al,1996), the results were good.

The basic feature of POM is briefly introduced as follows, 1) A second order turbulence closure model for the vertical viscosity, 2) sigma coordinate in the vertical with realistic bathymetry, 3) horizontal curvilinear coordinate and an Arakawa C scheme (Arakawa and Lamb, 1977), 4) the horizontal time differencing is explicit whereas the vertical differencing is implicit, 5) a free surface and a split time step, 6) complete thermodynamic and 7) horizontal diffusivity coefficients calculated by the Smagorinsky (1963) parameterization.

1.2.1. General information

The model domain extends from 117ºE to 131ºE, and from 24ºN to 41.5ºN, the model grid is 0.25º x 0.25°. The model grid and the positions of 81 stations are showed in Fig 1. For the vertical, 11 levels and real topography were used. The coefficient in horizontal eddy viscosity is chosen to be 0.1, and the external time step for gravity wave is 45 seconds while the internal time step is 15 minutes. The initial u=v=w-0, so called " cold start". Since the sea water density is assumed to be constant, the model results can be considered very close to winter circulation.

1.2.2. Open boundary conditions

At the open boundary, the elevation is specified. It contains two parts, one is the tide elevation, the sum of diurnal (K_1+O_1) and semidiurnal (M_2), the other is a mean elevation corresponding to the Kuroshio, which is obtained from geostrophic relation.

Concerning the transport of the Kuroshio, there are large differences in the values in the literature, ranging from 7 Sv to 80 Sv. Our experience suggests that two are more reliable: Chen et al (1992) and Kagimoto et al (1996). Chen et al's results of the Kuroshio transport southwest of Kyushin in Jan. 1986 is 30.0-32.0 Sv, Kagimoto et al estimated the averaged Kuroshio transport (from I 973 to I 992) through P-N line was approximately 25 Sv. In the present study, we set the Kuroshio Transport to be 30 Sv, it is acceptable. At the boundary, the Kuroshio countercurrent is considered. Since we have a cold start, the relax period of boundary conditions is I 5 days to avoid instability.

Since the present version of POM split the flow into internal and external modes, we describe the velocity boundary conditions separately as follows:

For the external mode, we require the normal velocities to satisfy the following radiation condition originally according to Flather (1976) and later converted to oceanography by Oey and Chen (1 992), Jia Wang et al (I 993).

$$V_{n,b}(l,t) = V(l,t) + (c/h)[E_{b-1}(L,t)-E_b(l,t)]$$

where b and b-1 denote the boundary point and the interior point, respectively. V(l,t) denotes the sum of mean transport and tide current; c, the local shallow water gravity wave speed. $E_b(l,t) = E_m + E_t$, where E_m is the mean elevation induced by mean transport mentioned above, and E_t is the tidal elevation.

For the internal mode, we also use radiation normal velocity boundary conditions given by Mellor (1996) in, formula (16-4).

1.3. Model results

In this paper, we call the model results general circulation under the conditions of tidal forcing and Kuroshio input. Of course, the density current and wind induced current are also important, especially in the Yellow Sea during summer when the Yellow Sea cold water mass appears.

In order to obtain the general circulation pattern. we have two runs, one is to put diurnal tidal forcing at open boundary and use interior observations as validation to test the POM; the other is to put all the tide observations as forcing. Since we focus on the ocean circulation, the later contains more real information and the results can be considered to be more realistic.

1.3.1. Tide modeling

Zhao B.R. et al (1994) did update tide research. For easy comparison we also select ml as the diurnal component as they did. Our procedure differs from theirs in two respects: the first is that we use turbulence closure model to calculate vertical viscosity and the second is that we consider the Kuroshio simultaneously.

We selected 81 stations evenly distributed along the entire coastline (Fig 1). The ml harmonic constant errors are listed in the following table (Table 1), the M_2 harmonic constant errors are showed in following paper. Our results are surprisingly accurate, this is much better than that in literature.

Although the diurnal harmonic constant errors of amplitude and phase (1.7 cm and 5.2º respectively) are small, the largest amplitude and phase errors still reach 8.6 cm (point 4) and 25.9º (point 22). The system phase errors exist along Shanghai and Fujian coastline. In order to get more reasonable results, we used all the tide harmonic constants as forcing in the following general circulation modeling.

1.3.2. General circulation patterns

After 100 days in the model, we used elevation data to do harmonic analysis, the cotidal charts of M_2 is shown in Fig 2. We selected layers 2, as representative of surface, layer. The corresponding daily-averaged current chart is shown in Fig 3.

The Kuroshio path: the modeled Kuroshio path and the change of current direction at 30.5ºN agree well with long-term observations. From 25ºN, a branch of the Kuroshio goes along the Taiwan coastline counterclockwise and then turns northeast, it rejoins the main current at 29ºN. This branch is called the Taiwan warm current in literature. It controls the whole southern part of the East China Sea (Guan B.X. and Chen S.J.,1962). It should be pointed out that there is a divergence zone around (28 N, 124.5 E) mainly due to a shelf-like topographic feature, with sharp dropoffs on 3 sides and rapidly ascending on the fourth side. This zone corresponds to upwelling and is helpful to the marine ecosystem. The existence of the divergence zone needs to be confirmed by further observations.

Tsushima warm current: About the origin of Tsushima warm current, there are mainly two viewpoints. The first is that Tsushima warm current is a branch of Kuroshio (Qiu and Inasato, 1990), the other is that it is multi-sourced (Wang , 1994). Our model results confirm the later viewpoint.

It is interesting that a current exists from the Sea of Japan to the study area through the Tsushima strait. From Fig. 3.6, some observed surface currents agree with the model results, but the observed surface current is not as steady as the model results. The track of drift buoy can also confirm our model results (Fig 4), we still think that this current needs much more study.

The current circulation of the Yellow Sea: Although there are many excellent papers about the Yellow Sea circulation (Li H. Q. and Yuan Y. L.,1993 ;Le K. T. and Mao H.L.,1 990), most of them concern the Yellow Sea cold water mass or infer circulation pattern from temperature and salinity distributions. As mentioned by Yuan Yeli et al (1 993) and Guo Bingiluo (1993), no observation can confirm that the origin of Yellow Sea warm current is the Tsushima current, its formation mechanism is still unclear. From our results, there is much difference between the circulation in the surface layer and the bottom layer. In the surface layer of south Yellow Sea, the currents go southward along the coastline at about 3-5 cm/s. In a narrow region off the Korean coast, a strong "warm" current (10-20 cm/s) goes northward (Qiu B, ea al, I 990). At the basin center, there is a weak clockwise vortex. In the surface layer of Northern Yellow Sea there is a weak clockwise vortex too. In summer, the density difference can not be neglected, so counterclockwise circulation of the surface layer does not appear in our model (Takahashi et al, 1995a). At the bottom layer of south Yellow Sea, a clockwise circulation dominates (Fig 3.5) and mainly goes northward in the basin middle area. This circulation is steady (Takahashi S. et al, 1995a,b). Along the coastline, the current goes southward and it is stronger off the Chinese coast. As in the surface layer, a narrow current goes northward off the Korean coast. This circulation pattern agrees with the observations and model results in literature. In winter, the northwest wind strengthens the southward coast current and the northward current in the middle area at the bottom layer. This is beyond the scope of this paper. The main defect of the present study is that temperature and salinity are fixed, so the surface currents of Kuroshio are smaller than observations in deep-sea area.

1.4. Conclusion

Based on POM, we simulated the general circulation of the East China Sea and the Yellow Sea the Kuroshio and tidal forcing are considered. Since the density is fixed, the surface Kuroshio current is smaller in deep sea area and the surface summer counterclockwise circulation pattern of the Yellow Sea mainly induced by the topographic heat accumulation effect (Takahashi S., 1995a) does not appear. Other patterns agree with the observations and model results in literature very well.

References

Arakawa A, VR Lamb. A description of the NCAR global circulation models, Comput. Pyhs.,17,173-265,1977.

Blumberg AF, GL Mellor. Diagnostic and prognostic numerical circulation studies of the South Atlantic Bight, J.Geophys. Res., 88, 4579-4592,1983.

Blumberg AF, GL Mellor. A description of a three-dimensional coastal ocean circulation model, Coastal and Estuarine Sciences 4:three-dimensional coastal ocean models, N.S.Heaps Ed., Amer.Geophys.Union. 1-16,1987a.

Bhlmberg AF,HJ Herring. Circulation modeling using orthogonal curvilinear coordinates, Three dimensional models of marine and estuarine dynamics, J.C.J. Nihoul and B.M.Jamart, Eds.,Elsevier Oceanogr. Ser., 45,55-88,1987b.

Chen C, RC Beardsley, R Limeburner. The structure of the Kuroshio southwest of Kyushu: velocity transport and potential vorticity fields, Deep Sea Res. ,39,245-268,1992.

Choi BH. A tidal model of the Yellow Sea and the East China Sea, KORDI, Report 80-2, Korea Ocean Research and Development Institute,72, 1980.

Choi BH. A three-dimensional model of the East China Sea, In: Ocean-Hydrodynamics of the Japan and East China Sea, Elsevier Oceanography Series, 1984,209-224.

Fang Guohong. Tide and tidal current charts for the marginal seas adjacent to China, C. J. of

Oceanology and Limnology,4(1), 1-16, 1986.

Flather RA. A tidal model of the northwest European continental shelf, Mem. Soc, R. Sci. Liege, Ser. 6, 10,141-164,1976.

Guan BX, Chen SJ. The circulation system of marginal seas adjacent to china, In: Reports of the nation-wide comprehensive ocean investigation,Ser.5, Chapter 6,1-45,1962.

Guo BH. Major feature of the physical oceanography in the Yellow Sea, J. Oceanogr. Huanghai Bohai Seas, 11(3), 7-18, 1993 .

Jia Wang, Lawrence AM, IL Grant Ingram. A three-dimensional numerical simulation of Hudson Bay Summer Ocean Circulation: Topographic gyres, separations and coastal jets, J. Physical Oceanogr., 2496-2514, 1993

Kagimoto T, Yamagata T. Seasonal transport variations of the Kuroshio: An OGCM simulation J.P.O., Jan 1997

Kaneko A, S Mizuno, W. Koterayama, RL Gordon. Cross-stream velocity structure and their downstream variation of the Kuroshio around Japan ,Deep Sea Res.,39,1583-1594,1992.

Kaneko A, N Gohda, W Koterayanra, M Nakamura, S Mizuno, H Furukawa. Towed ADCP fish with depth and roll controllable wings and its application to the Kuroshio Observation. J. Oceanogr. 49,383-395,1993.

Kawabe M. Variability of Kuroshio velocity assessed from the sea-level difference between Naze and Nishinoomote, J. Oceanogr. Soc. Japan,293-304,1988.

Kubota M, H Yokota,T Okamoto. Mechanism of the seasonal transport variation through the Tokara Strait, J. Oceanogr., 51,441-458, 1995 .

Le KT, Mao HL. Wintertime structures of temperature and salinity of the southern Huanghai Sea and its current system, C. J. Oceanol. Limnol. Sinica,21(6),505-515,1990.

Li HQ, Yuan YL, Theoretical study on the thermal structure and circulation pattern related to cold water mass of Yellow Sea, C. J. Oceanol. Limnol. Sinica, 23(1),7-13,1992

Mellor GL, T Yamada. Development of a turbulence closure model for geophysical fluid problem, Rev: Geophys. Space Phys., 20, 851-875,1982.

Mellor GL, AF Blumberg. Modeling vertical and horizontal diffusivities with the sigma coordinate system, Moll Weather Rev., 113 , 1379-1383, 1985 .

Mellor, GL, T Ezer, LY: Oey. The pressure gradient conundrum of sigma coordinate ocean models, J. Atmos.Oceanic Technol. , 11, 1126-1134,1994.

Mellor GL. Users guide for a three-dimensional primitive equations, numerical ocean model, Princeton University, 40pp, 1996 .

Oey LY, P Chen. A model simulation of circulation in the northeast Atlantic shelves and seas, J. Geophys. Res.,75 ,20087-20116, 1992

Qiao F, F Yue and Y Yeli, An ocean model's validation in the South China Sea, Acta Oceanologica Sinica, in press, 1996.

Qiu B, N Imasato. A numerical study on the formation of the Kuroshio counter current and the Kuroshio branch current in the East China Sea, Continent. Shelf Res.,10,165-184,1990.

Shen YJ, Y Anle. The three-dimensional tide current simulation of semi-diurnal component in the East China Sea, Report on ocean and liminology, 1, 1-11, 1985 .

Shen YJ. Numerical simulation of tide and tide current in the East China Sea, Report of Shangdong Ocean College , 10(3),28-35, 1980.

Smagorinsky J. General circulation experiments with the primitive equations.1: the basic experiment, Mon. Wea. Rev. , 91 ,99-164, 1963 .

Takahashi S, Yanagi T, A numerical study on the formation of circulations in the Yellow Sea during summer, UMI/MER, 33(3), 135-147, 1995 a

Takahashi S,Isoda Y, Yanagi T. A numerical study on the formation and variation of a clockwise circulation during winter in the Yellow Sea, J. Oceanogr., 51(1),83-98,1995b

Wang Z.J..A numerical modeling study of the source of the winter and summer Tsushima current (surface layer),J.Oceanogr. Huanghai Bohai Seas, 12(3) 13-1 9,1994.

Yuan Y, Guo B, Sun X, Physical oceanography in pan- Yellow Sea region, 11(3),1-6, 1993 .

Zhao BR, Fang GH and Ding WL. The tide and tidal current simulation of the East China Sea. the Yellow Sea and Bohai Sea.Acta Oceanologica Sinica, 16(5),1-10,1994.

Table 1 The modeled and observed harmonic constants of m_1

	longitude	latitude	a_0	a_m	Δa	θ_o	θ_m	$\Delta\theta$		longitude	latitude	a_0	a_m	Δa	θo	θm	$\Delta\theta$
1	123°9'E	39° 4'N	28.2	27.2	-1.0	313.7	315.3	1.6	42	126° 44'E	26°20'N	18.0	18.0	0.0	186.0	186.6	0.6
2	122°40'E	39°19'N	27.4	29.1	1.7	322.2	324.4	2.2	43	124°24'E	39°42'N	33.0	35.7	2.7	312.0	308.4	-3.6
3	121° 40'E	38° 56'N	23.0	20.2	-2.8	343.3	346.4	3.1	44	124° 16'E	39°48'N	34.0	36.2	2.2	311.0	310.1	-0.9
4	121° 0'E	40°43'N	32.1	40.7	8.6	80.6	85.3	4.7	45	123° 45'E	39°45'N	31.0	35.0	4.0	306.0	313.0	7.0
5	119° 37'E	39° 55'N	26.1	28.0	1.9	87.8	94.1	6.3	46	123°5'E	39°29'N	37.0	31.8	-5.2	319.0	319.9	0.9
6	117° 43'E	39° 6'N	31.8	29.0	-2.8	126.9	134.2	7.3	47	125°7'E	39°25'N	39.0	36.1	-2.9	314.0	302.7	-11.3
7	117° 36'E	38° 37'N	23.0	29.0	6.0	122.0	138.1	16.1	48	125°11'E	38°40'N	33.0	33.0	0.0	295.0	294.0	-1.0
8	120° 19'E	37° 39'N	17.9	17.0	-0.9	168.2	169.0	0.8	49	124° 47'E	38°11'N	29.0	31.0	2.0	282.0	288.4	6.4
9	121°24'E	37° 32'N	11.8	13.7	1.9	268.7	261.3	-7.4	50	125°20'E	37°45'N	33.0	32.3	-0.7	277.0	276.3	-0.7
10	122° 10'E	37° 30'N	16.7	16.7	0.0	283.5	277.3	-6.2	51	125° 33'E	37°44'N	33.0	33.1	0.1	278.0	275.0	-3.0
11	120° 45'E	38° 10'N	2.2	5.7	3.5	180.7	179.9	-0.8	52	126° 14'E	37°39'N	35.0	34.0	-1.0	277.0	279.6	2.6
12	122° 42'E	37°23'N	20.4	20.3	-0.1	290.0	287.5	-2.5	53	126° 34'E	37°30'N	35.0	34.3	-0.7	278.0	280.0	2.0
13	122° 25'E	36° 53'N	21.0	21.6	0.6	291.2	292.3	1.1	54	126°9'E	37°15'N	38.0	33.0	-5.0	261.0	272.2	11.2
14	121° 29'E	36° 48'N	22.0	24.0	2.0	308.1	302.0	-6.1	55	126° 27'E	37°2'N	35.0	33.8	-1.2	266.0	277.4	11.4
15	120° 19'E	36° 5'N	24.0	26.1	2.1	326.6	323.6	-3.0	56	126° 8'E	36°47'N	33.0	32.1	-0.9	259.0	257.5	-1.5
16	119° 33'E	35° 23'N	25.7	26.8	1.1	337.1	339.9	2.8	57	126° 26'E	36°23'N	33.0	32.3	-0.7	253.0	248.5	-4.5
17	119° 27'E	34° 45'N	26.6	27.0	0.4	343.7	346.0	2.3	58	126° 43'E	35°39'N	28.3	32.0	3.7	251.3	241.0	-10.3
18	119° 47'E	34° 29'N	24.5	25.9	1.4	352.0	350.3	-1.7	59	126° 1'E	35°21'N	28.0	27.2	-0.8	232.0	233.1	1.1
19	121° 37'E	32° 8'N	15.9	14.9	-1.0	117.5	102.3	-15.2	60	126° 5'E	35° 3'N	21.0	27.7	6.7	227.0	223.4	-3.6
20	122° 14'E	31° 25'N	19.6	18.8	-0.8	151.4	149.0	-2.4	61	126°1'E	34°34'N	25.0	25.4	0.4	215.0	209.0	-6.0
21	121° 54'E	31° 7'N	21.2	22.8	1.6	170.2	150.5	-19.7	62	126°16'E	34°23'N	27.0	25.1	-1.9	187.0	196.4	9.4
22	121° 22'E	30° 44'N	29.0	28.1	-0.9	190.6	164.7	-25.9	63	126°45'E	34°19'N	25.0	23.8	-1.2	173.0	180.9	7.9
23	122° 36'E	30° 49'N	22.3	21.6	-0.7	170.4	168.1	-2.3	64	127°9'E	34°30'N	24.0	23.8	-0.2	168.0	168.4	0.4
24	121° 5'E	30° 36'N	30.0	30.3	0.3	195.2	171.3	-23.9	65	127°45'E	34°44'N	17.0	19.9	2.9	153.0	150.7	-2.3
25	122 °18'E	30° 15'N	23.8	25.8	2.0	182.1	173.4	-8.7	66	128°3'E	34°43'N	16.0	17.0	1.0	146.0	146.3	0.3
26	122°4'E	30°0'N	25.6	27.5	1.9	191.6	174.5	-17.1	67	128°43'E	34°50'N	8.0	8.0	0.0	131.0	130.0	-1
27	122° 18'E	29° 57'N	25.1	26.0	0.9	196.4	177.0	-19.4	68	129°41'E	33°45'N	15.0	15.0	0.0	221.0	221.0	0.0
28	122°1'E	29° 49'N	25.0	27.9	2.9	188.4	177.0	-11.4	69	129°53'E	33°33'N	15.7	15.0	-0.7	225.1	224.6	-0.5
29	121° 57'E	29° 15'N	25.8	28.0	2.2	192.0	186.4	-5.6	70	129°33'E	33°23'N	19.0	22.4	3.4	209.0	210.5	1.5
30	121° 17'E	28° 5'N	26.9	27.3	0.4	200.2	199.4	-0.8	71	128°50'E	32°45'N	23.0	23.3	0.3	194.0	186.0	-8.0
31	120°48'E	27° 58'N	24.9	27.9	3.0	212.4	203.5	-8.9	72	129°7'E	32°59'N	18.0	24.0	6.0	194.0	189.7	-4.3
32	120°24'E	27° 10'N	27.1	27.4	0.3	211.0	209.9	-1.1	73	129°51'E	32°43'N	23.0	26.9	3.9	182.0	181.9	-0.1
33	121°10'E	26° 58'N	27.0	24.9	-2.1	214.7	205.9	-8.8	74	129°47'E	32°34'N	22.0	26.3	4.3	175.0	181.3	6.3
34	119°42'E	26° 1'N	25.0	28.2	3.2	226.8	224.0	-2.8	75	130°1'E	32°12'N	23.0	25.1	2.1	185.0	178.7	-6.3
35	119°59'E	25° 27'N	27.9	25.9	-2.0	231.5	229.7	-1.8	76	129°51'E	31°51'N	26.0	24.6	-1.4	179.0	178.0	-1.0
36	121°45'E	25°9'N	17.0	18.0	1.0	213.5	196.0	-17.5	77	130°13'E	31°17'N	23.0	24.1	1.1	174.0	175.1	1.1
37	121° 52'E	24° 35'N	18.0	17.9	-0.1	207.5	205.7	-1.8	78	129°51'E	29°50'N	19.0	19.3	0.3	172.0	170.3	-1.7
38	123° 41'E	25° 56'N	20.0	19.0	-1.0	198.5	196.0	-2.5	79	129°12'E	29°9'N	19.0	19.5	0.5	187.0	181.7	-5.3
39	123° 0'E	24° 25'N	17.0	17.0	0.0	200.0	200.0	0.0	80	127°58'E	27°3'N	18.0	18.0	0.0	191.0	188.6	-2.4
40	125° 18'E	24° 48'N	16.0	16.0	0.0	214.0	213.3	-0.7	81	127° 18'E	26 °13'N	18.0	18.0	0.0	190.0	187.8	-2.2
41	124° 10'E	24° 20'N	19.0	19.0	0.0	202.0	202.0	0.0		mean	absolute	errors		1.7			5.2

a_0: observed amplitude of m_1; a_m : modeled amplitude of m_1;

θ_0: observed phase of m_1; θ_m : modeled phase of m_1

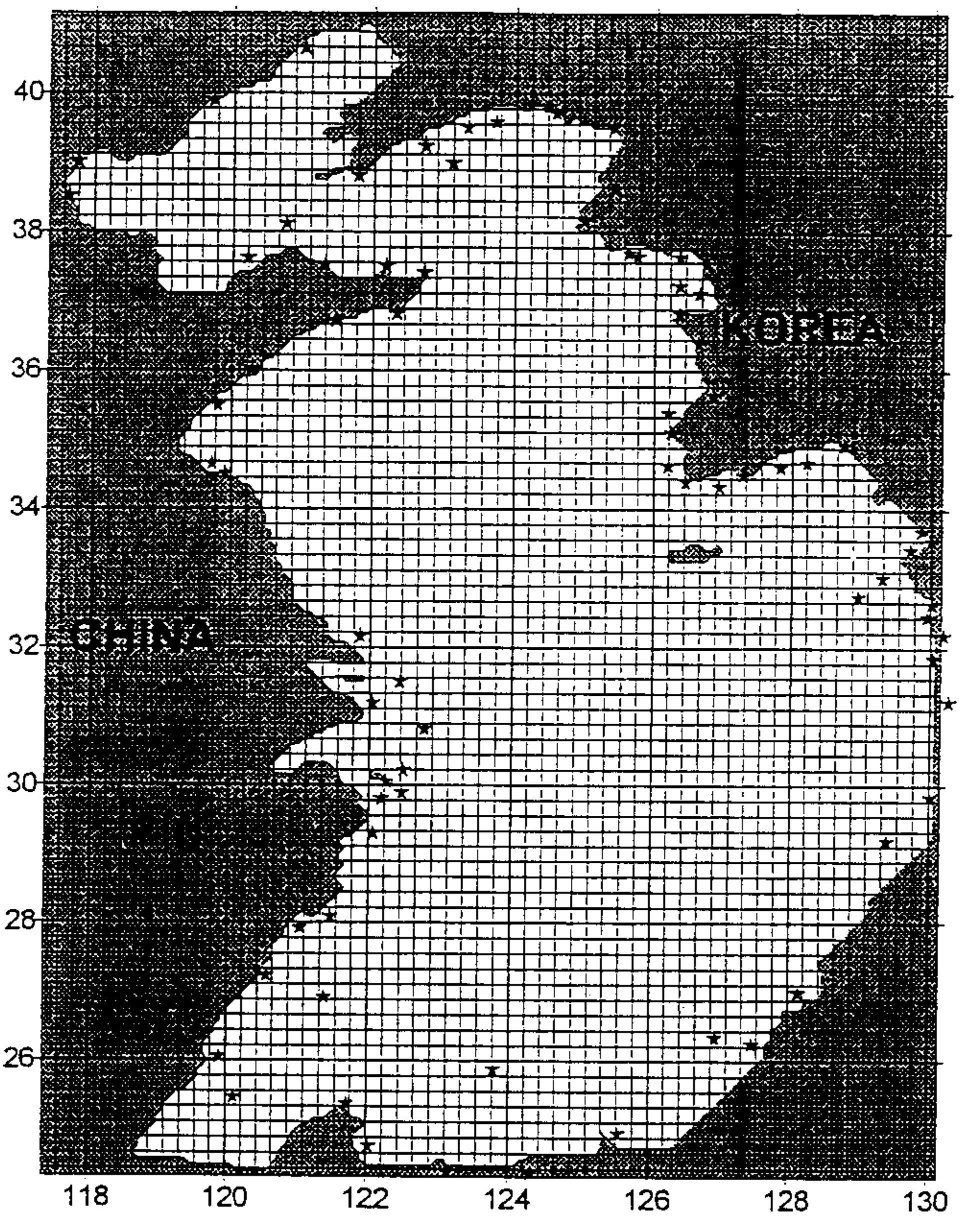

Fig 1 The chart of study area and model grid (★ represents station of sea level observation)

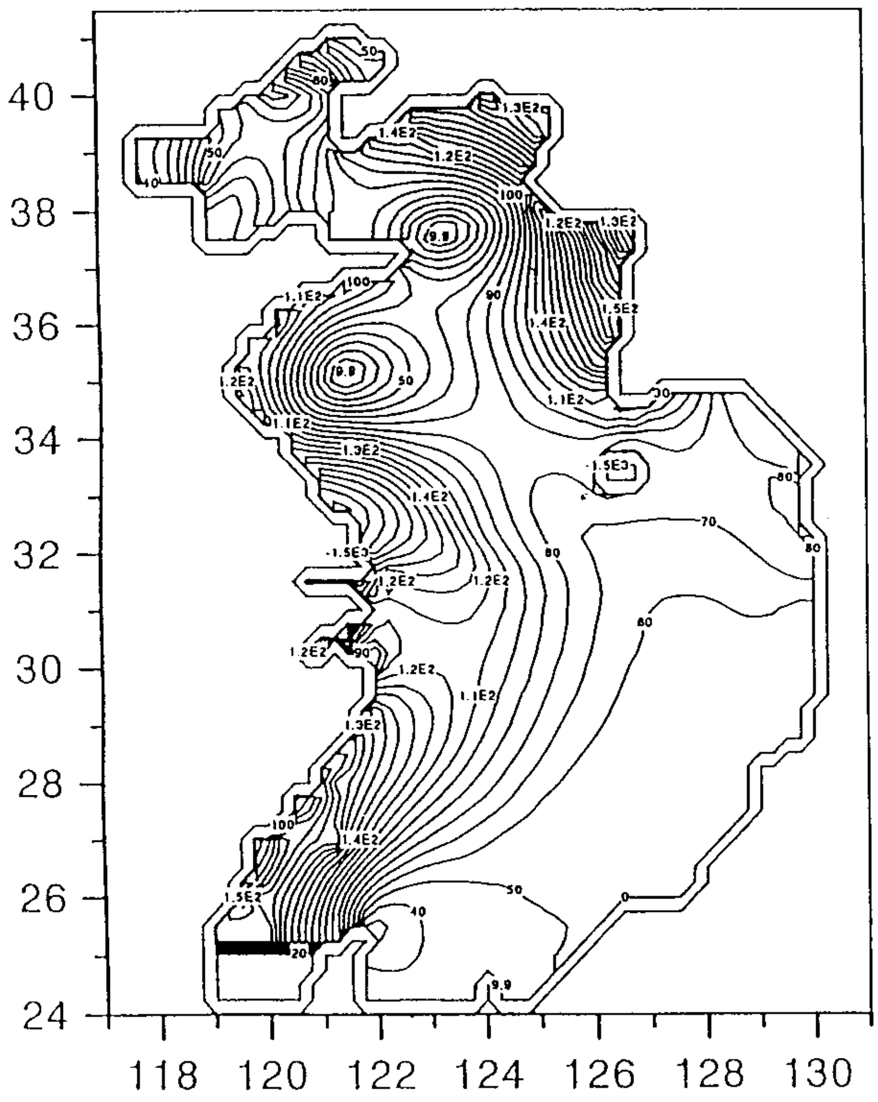

Fig. 3.2a The amplitude distribution of M2

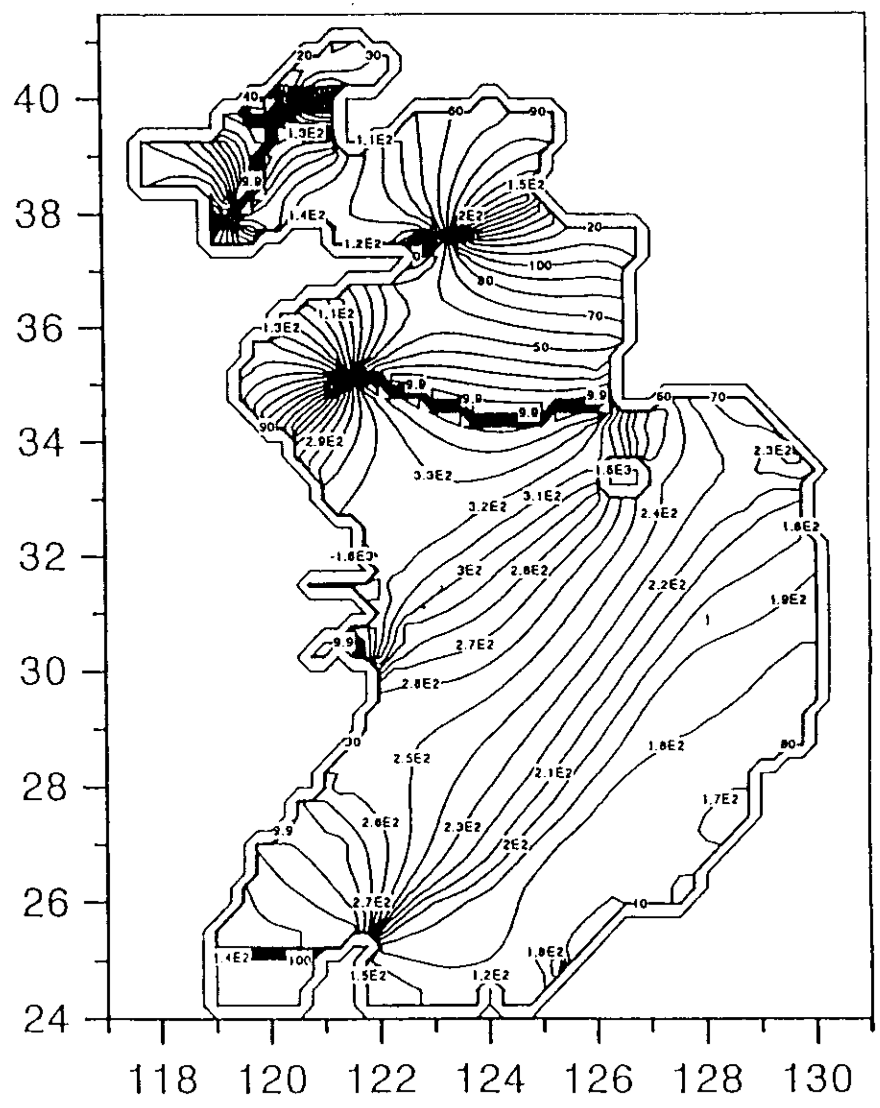

Fig. 3.2b The phase distribution of M2

Fig. 2 The cotidal chart of M2

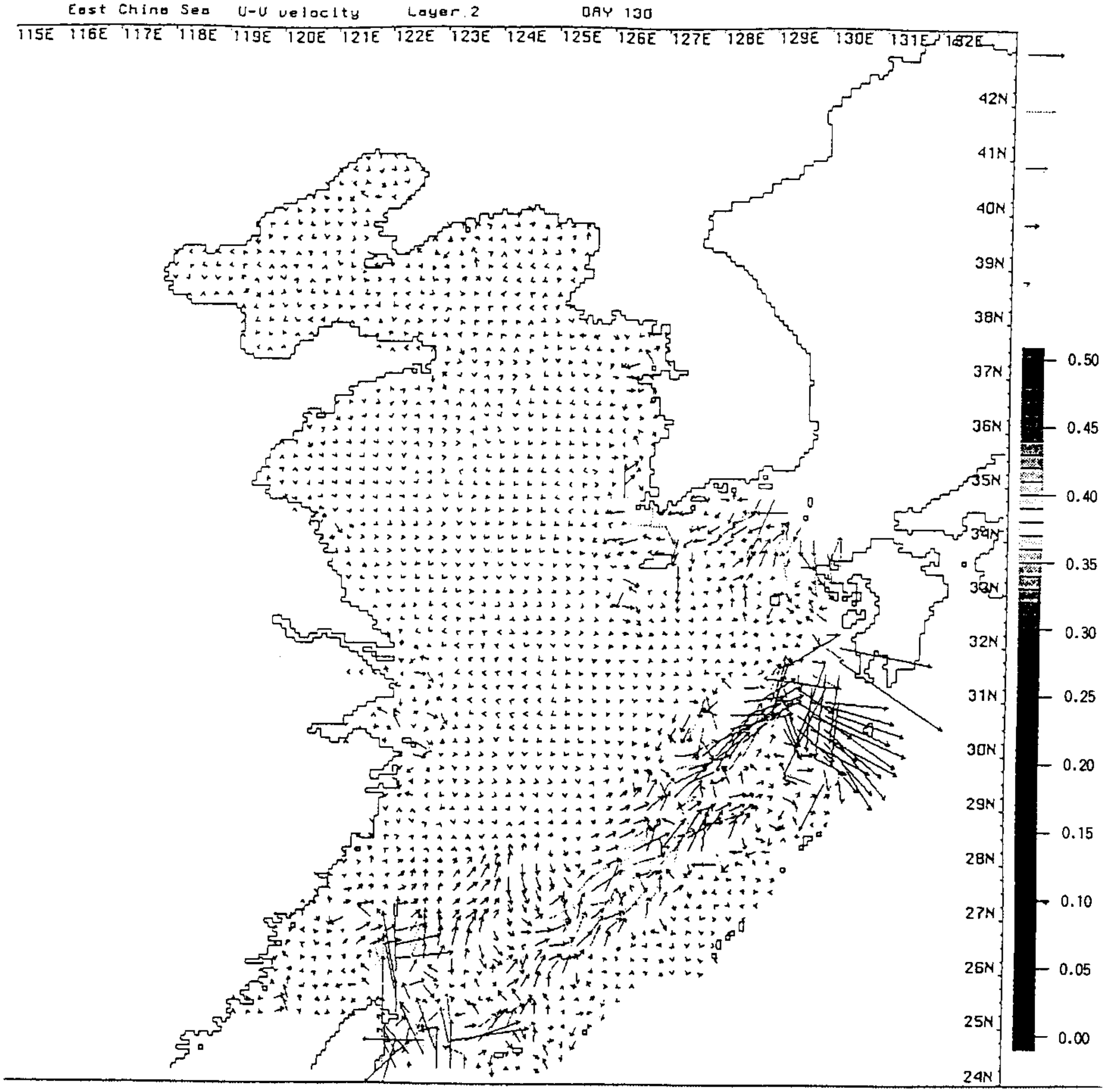

Fig 3 the current distribution of surface layer

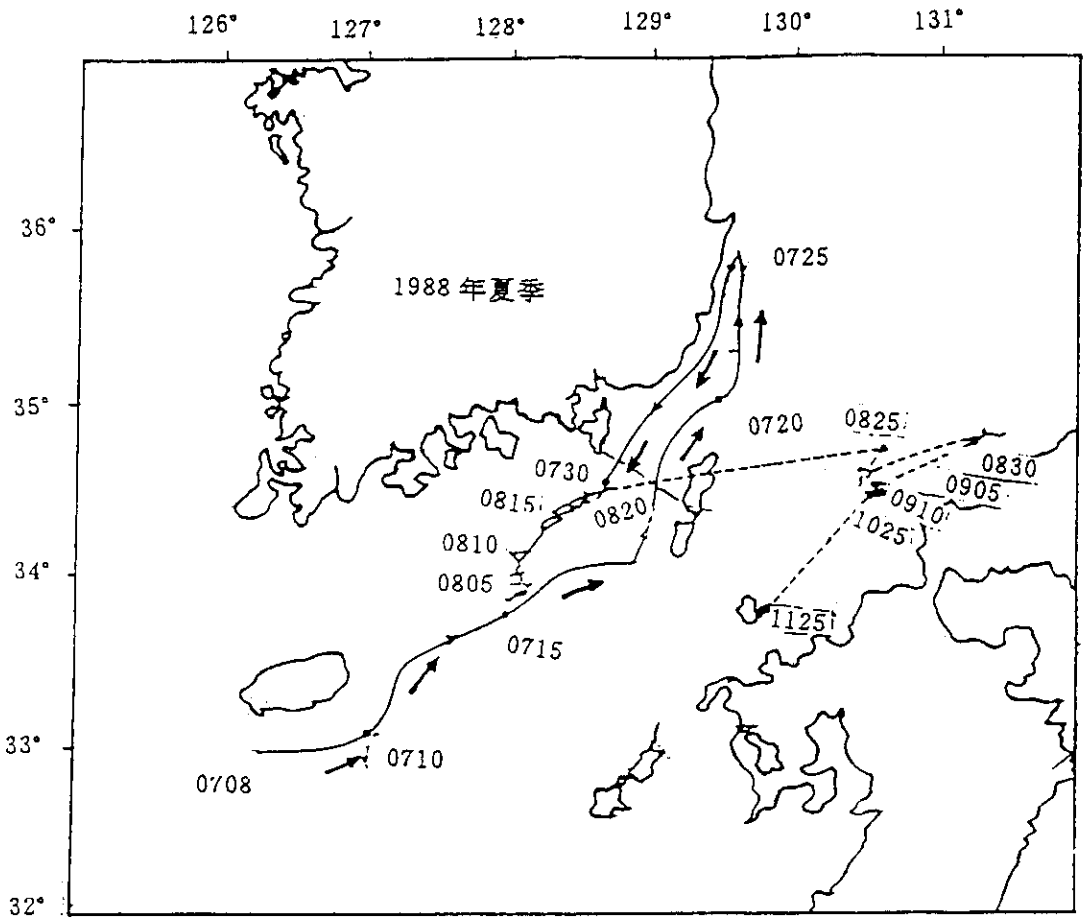

Fig. 4 The track of drift buoy (from the China—Korea cooperation)

2. Horizontal 2-D simulation of sediment transport in the Changjiang Estuary

2.1. Introduction

Silt and mud covers Changjiang estuary and these materials are easy to be suspended and transported under the actions of tidal currents and wind waves. Every year the sediment carried by flow stream down the sea averages 486 million kg and a part of them deposit on the estuary area. There are both suspended sediments and bed loads that move to and for as well as exchange unceasingly with the materials in sea bed. At present, the navigation channel has to be dredged every month to guarantee -7.0 m bed elevation due to the sediment silt, even so, the channel can not meet the needs of the economic development in China.

In this report an attempt is made to present a horizontal 2-D mathematical model of sediment transport in the estuary. The actions of tidal currents and wind waves, the effect of salinity to the suspended load have been considered. The movement of both suspended and bed loads has been simulated. The scouring and silting of sediment, especially bed load, have been reflected through one-month tidal current calculations in flood season and dry season respectively. On the basis of verifying the field data observed in the estuary, the quantity of silt in navigation channel is predicted by this model after the project completed.

2.2. Numerical Model

2.2.1. The Model of Unsteady Flow

Under the orthogonal curvilinear coordinate system, the basic equations of 2-D unsteady flow motion can be written as follows

$$\frac{\partial \zeta}{\partial t}+\frac{1}{g_\xi g_\eta}\frac{\partial}{\partial \xi}(Hug_\eta)+\frac{1}{g_\xi g_\eta}\frac{\partial}{\partial \eta}(Hvg_\xi)=0 \qquad (1)$$

$$\frac{\partial u}{\partial t}+\frac{u}{g_\xi}\frac{\partial u}{\partial \xi}+\frac{v}{g_\eta}\frac{\partial u}{\partial \eta}+\frac{uv}{g_\xi g_\eta}\frac{\partial g_\xi}{\partial \eta}-\frac{v^2}{g_\xi g_\eta}\frac{\partial g_\eta}{\partial \xi}+g\frac{u\sqrt{u^2+v^2}}{C^2H}-fv$$
$$+\frac{g}{g_\xi}\frac{\partial \zeta}{\partial \xi}=\nu\left(\frac{1}{g_\xi}\frac{\partial A}{\partial \xi}-\frac{1}{g_\eta}\frac{\partial B}{\partial \eta}\right) \qquad (2)$$

$$\frac{\partial v}{\partial t}+\frac{u}{g_\xi}\frac{\partial v}{\partial \xi}+\frac{v}{g_\eta}\frac{\partial v}{\partial \eta}+\frac{uv}{g_\xi g_\eta}\frac{\partial g_\eta}{\partial \xi}-\frac{u^2}{g_\xi g_\eta}\frac{\partial g_\xi}{\partial \eta}+g\frac{v\sqrt{u^2+v^2}}{C^2H}+fu$$
$$+\frac{g}{g_\eta}\frac{\partial \zeta}{\partial \eta}=\nu\left(\frac{1}{g_\xi}\frac{\partial B}{\partial \xi}+\frac{1}{g_\xi}\frac{\partial A}{\partial \eta}\right) \qquad (3)$$

where

$$A=\left[\frac{\partial ug_\eta}{\partial \xi}+\frac{\partial vg_\xi}{\partial \eta}\right]/g_\xi g_\eta, B=\left[\frac{\partial vg_\eta}{\partial \xi}+\frac{\partial ug_\xi}{\partial \eta}\right]/g_\xi g_\eta$$

$$g_\xi=\sqrt{x_\xi^2+y_\xi^2}, g_\eta=\sqrt{x_\eta^2+y_\eta^2}$$

u and v are the depth-averaged components of velocity in the directions of ξ and η respectively, ζ is water surface level and H is water depth; g_ξ, g_η are Lami coefficient; f is Coriolis parameter; ν is turbulent viscosity coefficient.

2.2.2. The Model of Suspended and Bed Sediment Transport

(1) Non-equilibrium Suspended Load Transport Equation

Under the orthogonal curvilinear coordinate system, the basic equation of 2-D suspended load transport established by Dou Guoren [1] is

$$\frac{\partial(HS)}{\partial t} + \frac{1}{g_\xi g_\eta}\left[\frac{\partial(HUSg_\eta)}{\partial \xi} + \frac{\partial(HVSg_\xi)}{\partial \eta}\right] + \alpha\omega(S - S_*) = 0 \qquad (4)$$

where S is depth-averaged concentration of suspended sediment; α is an undetermined coefficient which can be determined by verification calculation; ω is falling velocity of sediment; S_* is the sediment transport capacity.

According to Dou Guoren's formula, the sediment transport capacity of tidal currents and wind waves has the following form [2]:

$$S_* = \alpha_0 \frac{\gamma\gamma_s}{\gamma_s - \gamma}\left[\frac{(u^2+v^2)^{3/2}}{C^2 H\omega} + \beta_0 \frac{H_w^2}{HT\omega}\right] \qquad (5)$$

where γ and γ_s are the unit volume weight of sea water and sediment particles respectively; H_w is the mean wave height and T is mean wave period; The Chezy coefficient C can be determined by Maning's formula

$$C = \frac{1}{n} H^{1/6}$$

where n is the roughness of seabed, in a common case n=0.012-0.025. According to the field measurements and wave flume data, we can take α_0=0.023 and β_0=0.0004 .

(2) Non-equilibrium bed load transport equation

The Non-equilibrium bed load transport equation derived recently by Dou Guoren is following form

$$\frac{\partial(\beta hN)}{\partial t} + \frac{\partial(\beta hNv_x)}{\partial x} + \frac{\partial(\beta hNv_y)}{\partial y} + \alpha_b\omega_b(N - N^*) = 0 \qquad (6)$$

where βh is the thickness of bed loads transport layer; N is the quantity of bed loads in the unit volume; α_b is the settling coefficient of bed load; ω_b is the falling velocity of bed load particle; N^* can be determined by

$$N^* = \frac{q_b^*}{\beta h v}$$

where q_b^* is the unit width transport capacity of bed loads in unit time.

Under the orthogonal curvilinear coordinate system, the equation mentioned above can be written as follows

$$\frac{\partial(hN)}{\partial t} + \frac{1}{g_\xi g_\eta}\left[\frac{\partial(huNg_\eta)}{\partial \xi} + \frac{\partial(hvNg_\xi)}{\partial \eta}\right] + \frac{\alpha_b}{\beta}\omega_b(N - N^*) = 0 \qquad (6)'$$

in which q_b^* can be determined by Dou's formula of bed load transport capacity

$$q_b^* = \frac{k_2}{C^2}\frac{\gamma\gamma_s}{\gamma_s - \gamma} m \frac{(u^2+v^2)^{3/2}}{\omega_b} \qquad (7)$$

where

$$m = \begin{cases} \sqrt{u^2+v^2} - V_K & V_K \le \sqrt{u^2+v^2} \\ 0 & V_K > \sqrt{u^2+v^2} \end{cases}$$

V_K is the critical velocity for the incipience of bed load particle and expressed by Dou as follows

$$V_k = 0.265\ln(11\frac{H}{\Delta})\sqrt{\frac{\gamma_s - \gamma}{\gamma} g d_{50} + 0.19(\frac{\gamma_0}{\gamma_0'})^{2.5}\frac{\varepsilon_K + gh\delta}{d_{50}}} \qquad (8)$$

where γ_0 is the dry unit volume weight of bed material; γ_0' is the stability dry unit volume weight of bed load material; *d50* is the median diameter of bed load particle; ε_K is the parameter of cohesive forces (for natural sand $\varepsilon_K = 2.56\ cm^3/s^2$). δ is the thickness of water film $\delta = 0.21\times10^{-4}cm$. Δ is the roughness height of bed

$$\Delta = \begin{cases} 0.5mm & d_{50} \le 0.5mm \\ d_{50} & d_{50} > 0.5mm \end{cases}$$

k_2 is a coefficient; ω_b is the settling velocity of particle; C is the Chezy coefficient. To fine send $\gamma_0 = \gamma_0'$.

(3) Seabed Deformation Equations

The equation of seabed deformation caused by suspended load is

$$\gamma_0 \frac{\partial \eta_s}{\partial t} = \alpha\omega(S - S_*) \tag{9}$$

where η_s is the thickness of silt or scour caused by suspended load.

The equation of seabed deformation caused by bed load is

$$\gamma_0 \frac{\partial \eta_b}{\partial t} = \alpha_b \omega_b (N - N^*) \tag{10}$$

where η_b is the thickness of silt or scour caused by bed load.

The total thickness of seabed silt or scour caused by both suspended load and bed load is

$$\eta = \eta_s + \eta_b$$

2.3. The Verification of Numerical Model

In order to predict the silt in the channel after the project of developing the north trough deep-water channel is completed, the numerical model must be verified with the data measured in the natural conditions.

2.3.1 Computational Domain

Owing to the boundary shape of Changjiang estuary is comparatively complicated, orthogonal curvilinear grids are adopted to fit the river channel and two dikes to be constructed. The studied region is given in Fig.1. The length is 200 km from west to east and the width is 130 km from north to south. The mesh number is 9430 and the mesh steps vary in size between 150m and 1500m depending on the topographical features (Fig.2).

2.3.2 Tidal Currents and Sediments

The data about the velocities and directions of tidal currents, the tidal levels and the sediment concentrations measured in February, March and September 1996 respectively are adopted to compare with the values of calculation. The survey points are showed in Fig.3 and Fig.4 for flood season and dry season respectively.

The comparisons between the calculated and measured values are given in Fig.5 and Fig.6. It can be seen that the calculated values are in good agreement with the measured data. The character of tidal pattern, shuttling inside the estuary and rotating outside the estuary, has been reflected in the model. The verification of sediment concentration in spring tide, middle tide and neap tide during flood and dry season have been done on the basis of the model of tidal currents. The concentrations in a tidal period at every measured station can be solved from the model of suspended load transport. The comparisons of the model results with the field data are satisfactory (Fig.7 and Fig.8).

2.3.3 The Verification of Seabed

The seabed deformation verification of scour and silt in the south trough and the north trough area is done by use of the topography surveyed in 1995 and in 1996 respectively.

Based on the tidal level surveyed in one month during flood and dry season, the scouring and silting thickness of suspended and bed load in one year at the position in Fig.15 has been obtained from the model of total sediment transport. The verification result is shown in Fig.16. Each line in the figure except line E has similar tendency to the actual one. The silt in the upper part of line E is calculated and it is equal to 9,310,000 m^3 that is close to the dredging quantity in every year. In the lower part of the north trough there is no dredging and the seabed elevation is the same as the measured one. The above-mention indicates the total sediment transport model can simulate the seabed deformation of scour and silt from the south side of the south trough to the north side of the north trough. Therefore the model can be used to predict the variance of sediment scour and silt after the regulation project is built.

2.4 Summary

In order to reply the quantity of sediment silt in the feasibility study of Changjiang estuary deepwater channel project, a 2-D total sediment transport model under the actions of tidal currents and wind waves has been established. The model is on the basis of the non-equilibrium suspended load and bed load transport equations derived by Dou Guoren. The orthogonal curvilinear grids have been adopted to fit the boundaries of channel and project. A lot of verification about tidal levels, velocities, and sediment concentrations in a tidal period have been done making use of the data measured in spring, middle and neap of flood and dry season respectively. The satisfactory results have been given by all of the verification and there is a similarity between the prototype and the model.

References

Dou Guoren, Dong fengwu, Dou Xiping, Li Tilai, Mathematical modeling of sediment transport in estuaries and coastal regions, Science in China (Series A), Vol.38 No.10, October 1995.

Dou Guoren, Dong fengwu, Dou Xibing, Sediment Transport of Tidal Currents and Waves, Chinese Science Bulletin, Vol.40 No.13, July 1995.

Dou Xiping, Numerical model study of suspended sediment transport in the deepwater channel of Changjiang estuary, the research report of Nanjing Hydraulic Research Institute, No.9506.

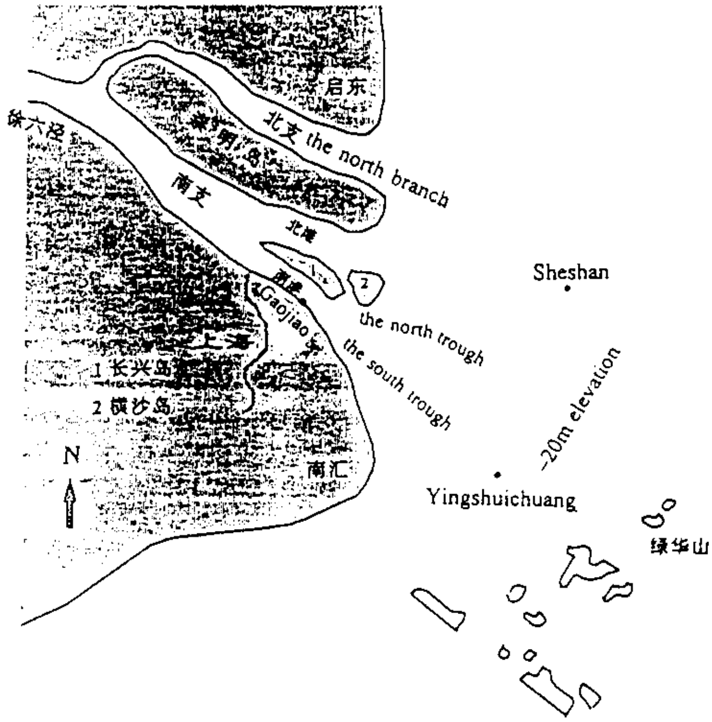

Fig. 1 Changjiang Estuary

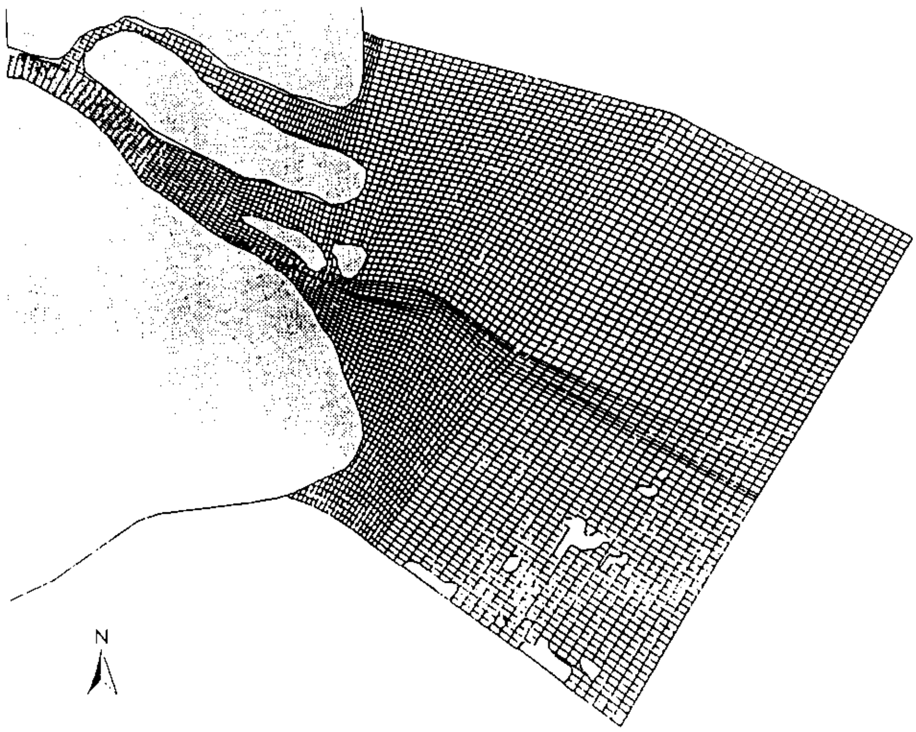

Fig. 2 the Calculation Mesh

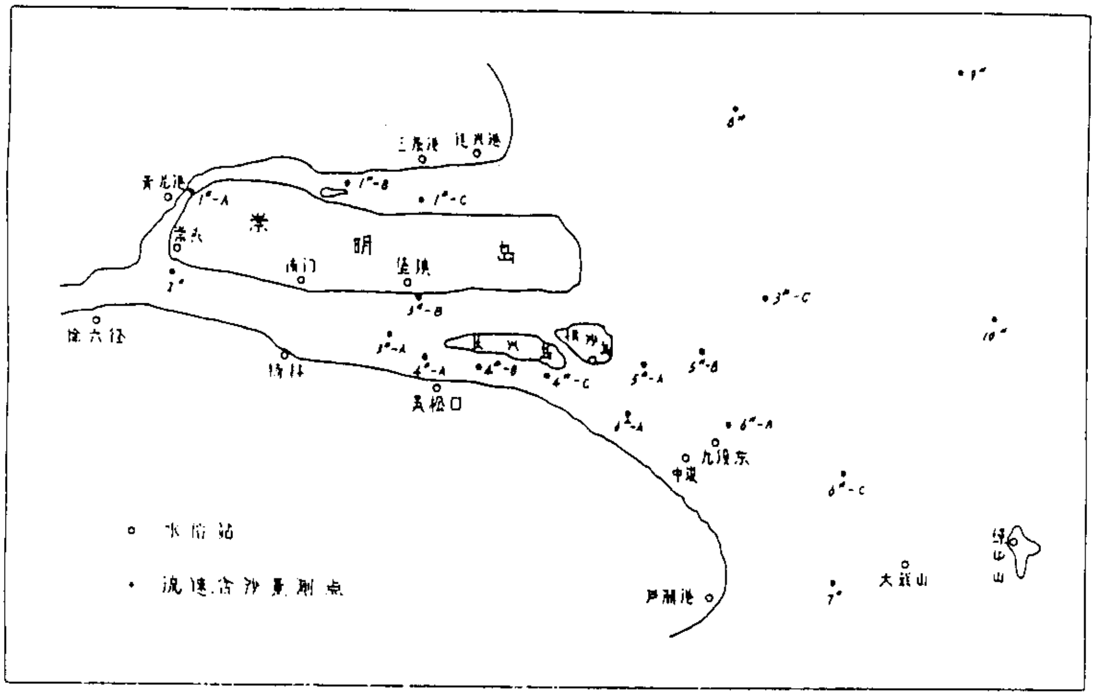

Fig. 3　the Measurement Stations in Dry Season

(1996. 2. 15-3. 15)

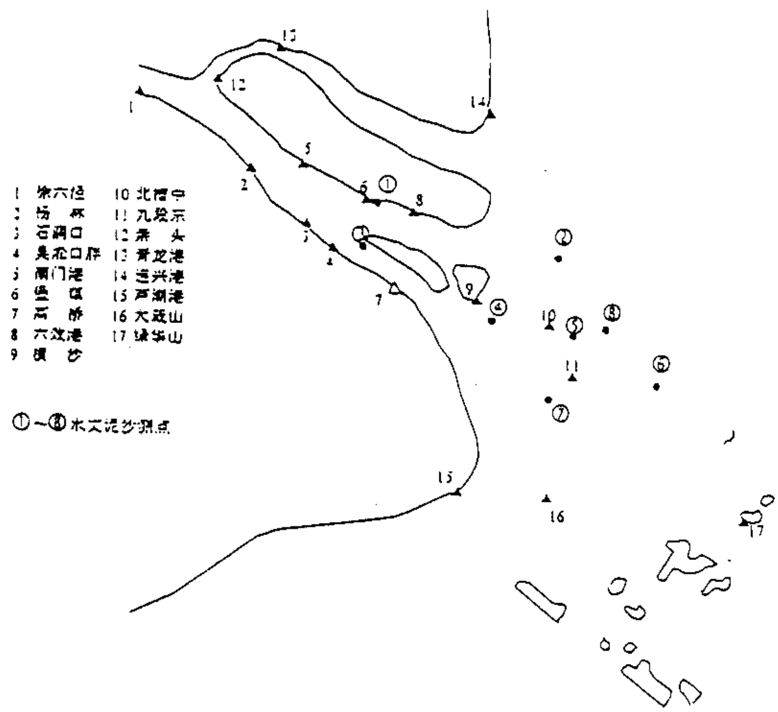

Fig. 4 the Measurement Stations in Flood Season

(1996. 9. 1-9. 30)

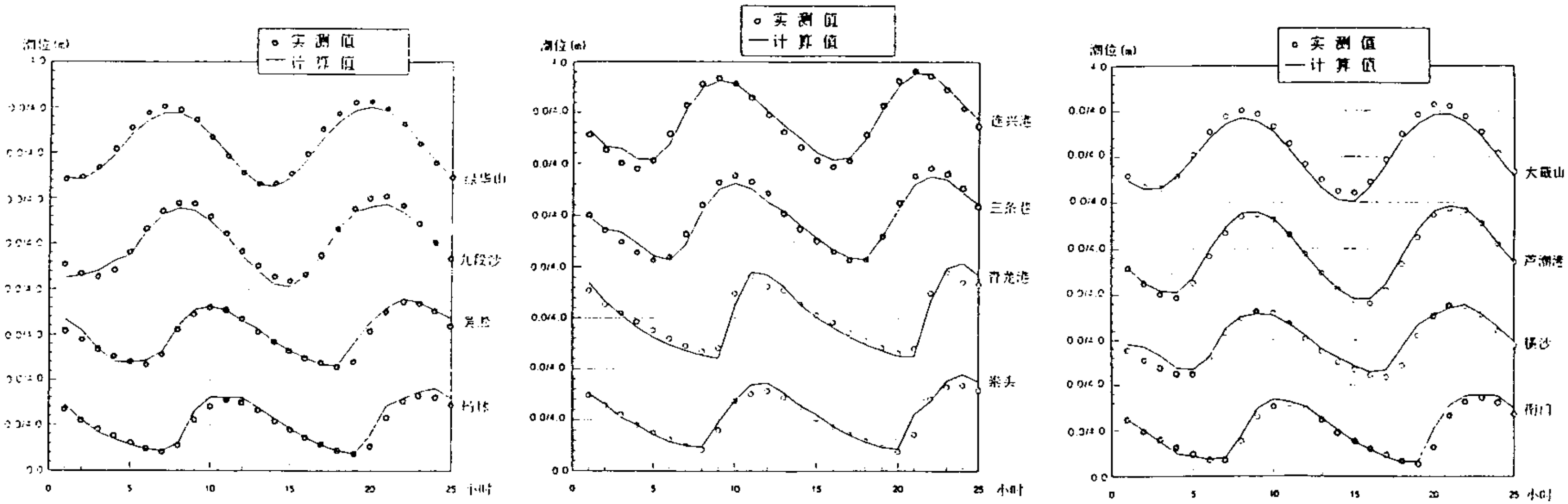

Fig. 5 the Verification of Tidal Level in Dry Season (Spring)

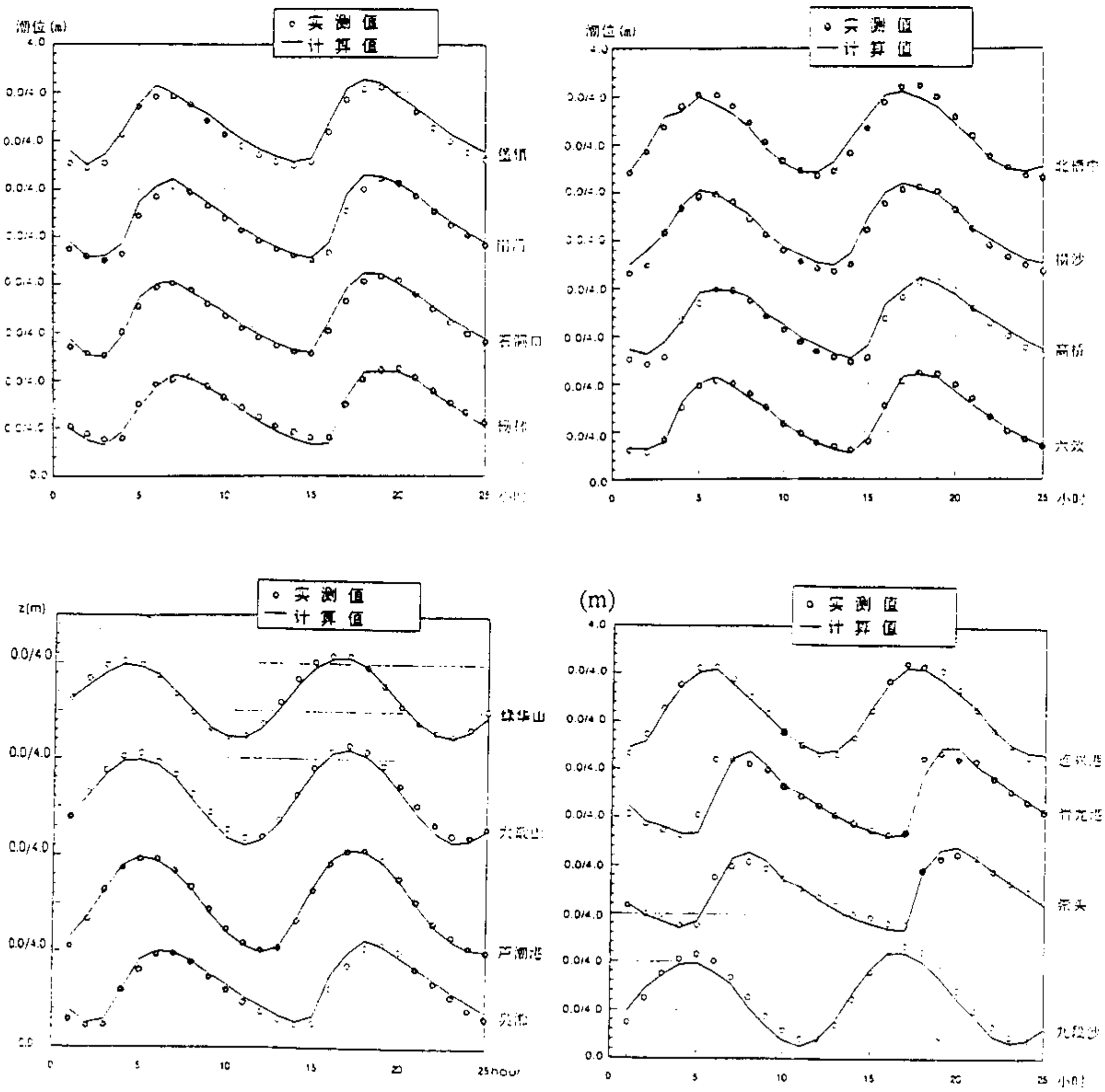

Fig.6. the Verification of Tidal Level in Flood Season (Spring)

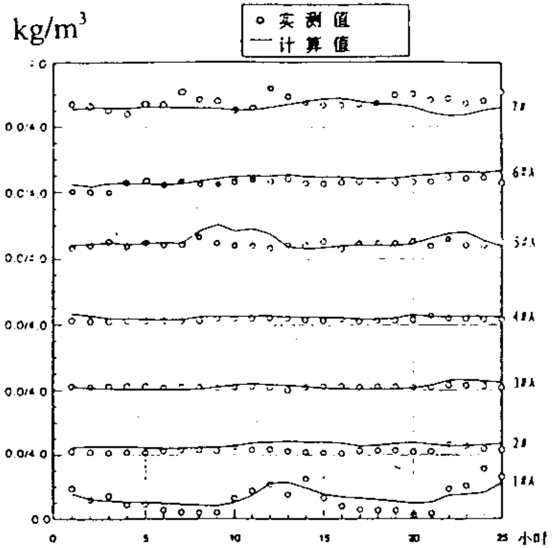

(Spring)

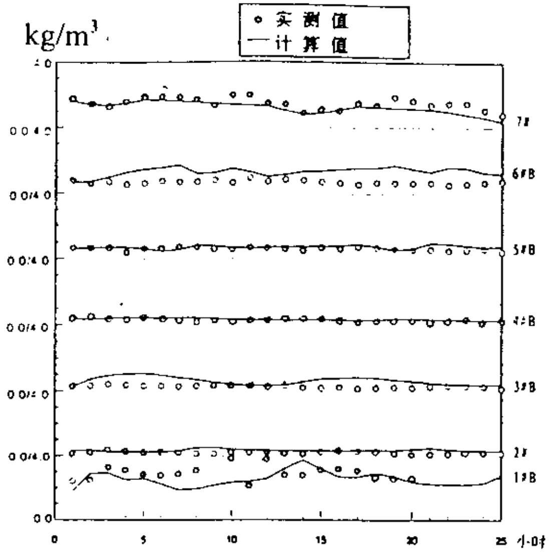

(Middle)

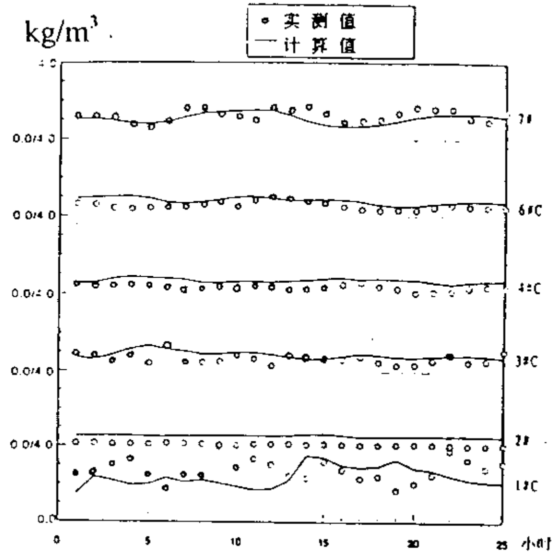

(Neap)

Fig. 7. the Verification of Concentration in Dry Season

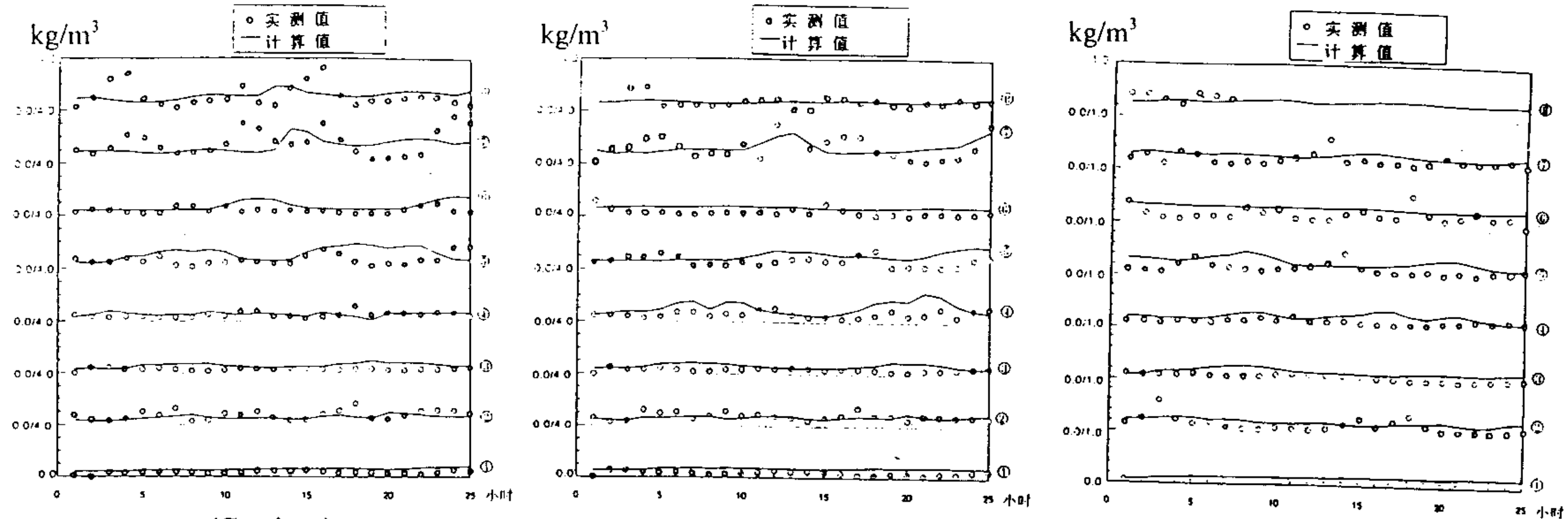

(Spring) (Middle) (Neap)

Fig. 8. the Verification of Concentration in Flood Season

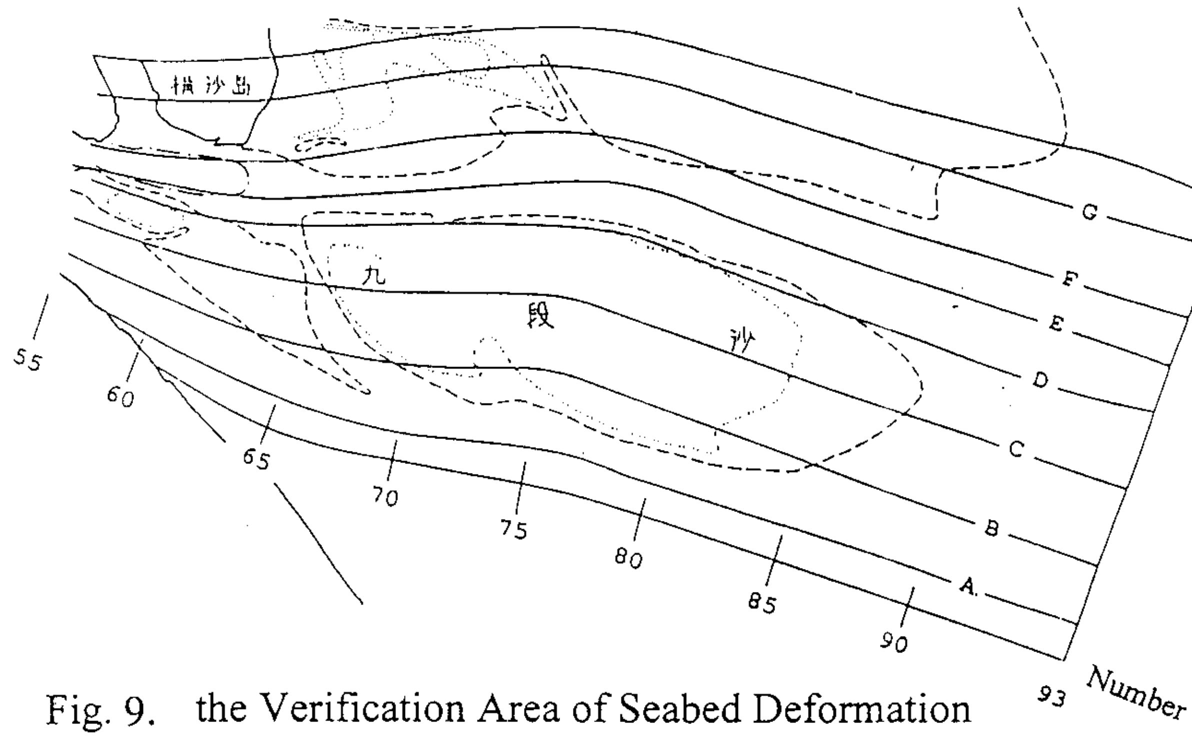

Fig. 9. the Verification Area of Seabed Deformation

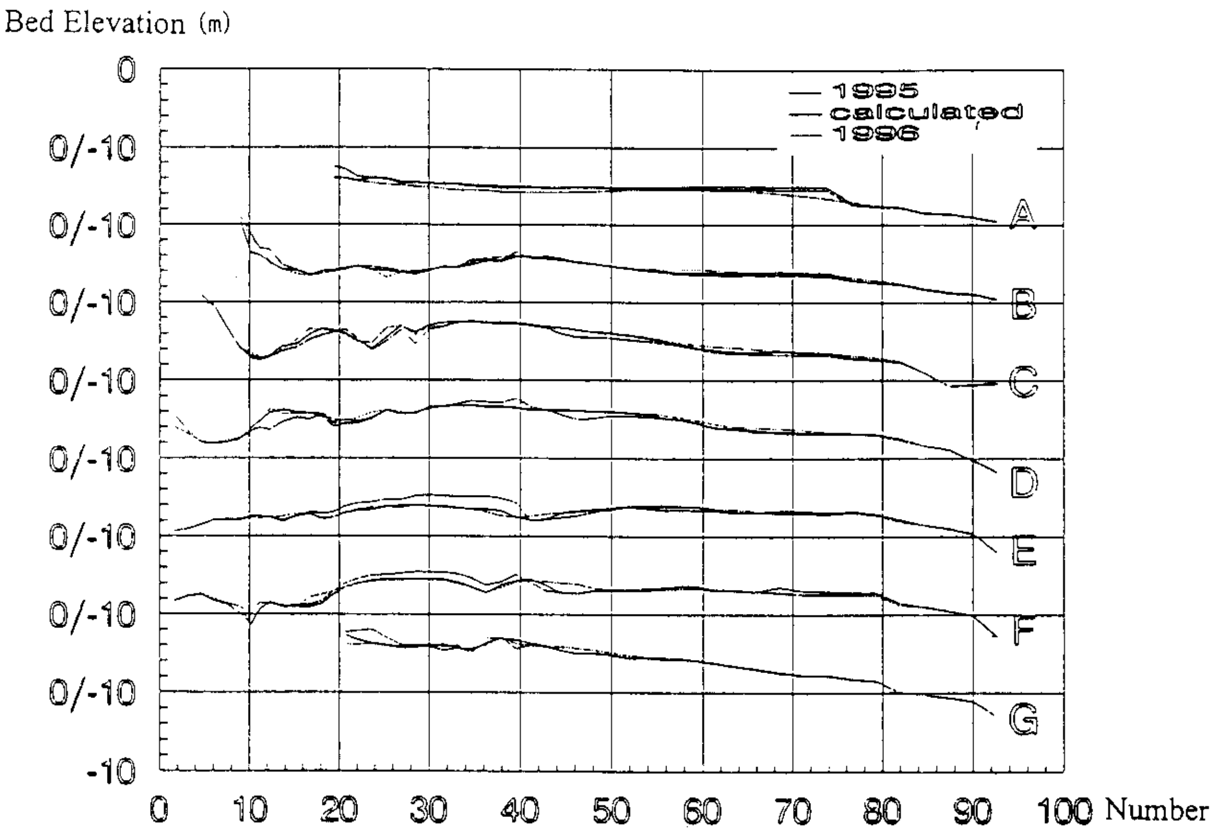

Fig.10 the Verification Result of Seabed Deformation

3 Organochlorine pesticides in sediment in the Changjiang Estuar

3.1 Introduction

Organochlorinated pesticides (e.g. DDT, BHC) accumulate in biota of all trophic levels and residues in water and sediments are reported in environmental compartments from all geographical latitudes (Preston, 1988; Everaarts, et al., 1993; Bignert et al , 1998, Iwata et al, 1994). They are ubiquitous toxic contaminants, due to their bioaccumulative capacity and highly persistence and specific physico-chemical properties in the environment (WHO, 1979;WHO, 1989). The organochlorinated pesticides were prohibited by most of countries in the world since the early 1980s. But it is of high stability and persistence as well as delay effect transported by soil and water, its effect may exists for several decades years on marine environment and ecology.

The Changjiang River drainage is a strong agricultural sector and agricultural practices in this drainage have resulted in non-point source contamination by several first-generation organochlorine pesticides, which is cheaper and efficient, before mid of 1980s. These organochlorine pesticides are transported from farmlands via soil erosion and agricultural runoff through branch-river into the Changjiang River. Finally, these compounds are eventually dispersed throughout the estuary to become incorporated into estuary sediments and accumulated in the lipophilic tissue of biota (Sheng, 1997, Lin, 1987). DDT and BHC residues were probably widespread in the Changjiang Estuary sediments deposited since the 1950s.

The aim of this study is to determine the current levels of organochlorine compounds in sediments of the Changjiang Estuary, and to reconstruct the organochlorine pollution history of the Changjiang Estuary by measuring pesticides concentrations in a sediment core dated with Pb210.

3.2 Materials and Methods

3.2.1 Sampling description

The location of sample stations show in Fig. 1. The short cores of C1 and Meso were taken from the Changjiang estuary in Oct 1997. The short cores of A1, A3, B3, C3 and Meso-2 were

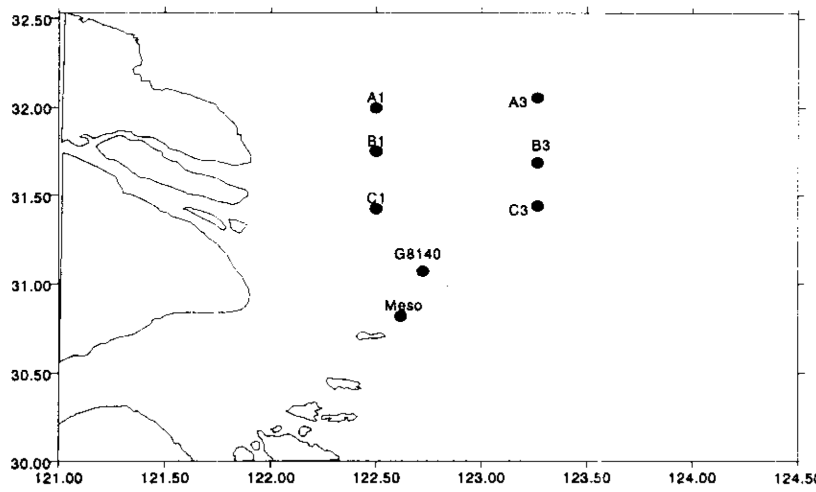

Figure 1. The sampling station location of sediments in the Changjiang Estuary

taken from the Changjiang estuary In June 1998. The surface samples were taken 0~2cm of top sediment then divided the core layer sediment per 2 and 5 cm. All samples were dried in natural condition and grilled to past 80 mesh. A long core of B1 (length 160cm, diameter 7.5cm) was taken using gravity tube sampler in June 1998 (water depth about 15m). The core was divided to three short cores and sealed, carefully removed, and frozen in a vertical position. The core was then cut into approximately 2.0cm vertical slices. Sediment the samples were freeze-dried before further analysis. Pb210 activity was determined to date the sedimentation rate.

3.2.2 Analysis

BHC and DDT in sediments were extracted by mixer hexane of acetone (v/v=1:1). Samples of B1, C1 and Meso, which were taken in Oct 1997, were extracted by Soxhlet method, then extracted solution was evaporated by a rotary evaporator and determined by GC-7AG gas chromatography (Shimaze Co. Ltd.) equipped with 63Ni electrode capture detector (ECD). The B1 long core samples and other surface sediments taken in June 1998 were extracted by accelerated solvent extraction (ASE-200, Dionex Co. Ltd.) with mixing solvent of acetone and n-hexane (pesticide quality, v/v=1: 1). The solvent in the extracts was dry up with N2, then dissolved to 5ml n-hexane, and analyzed on a HP gas chromatography-ion trap mass spectrometer system using a 30-m DB5-MS capillary column.

3.3 Results and discussion

3.3.1 Effect of organochlorine pesticides on marine environment of the Changjiang Estuary

In China, the first generation organochlorine pesticides (mainly DDT and BHC) began to be produced in 1952 and stopped producing and using in 1984, the annual production shows in Fig 1. Total about 9×10^6 tones DDTand 4.5×10^6 tones BHC were produced and used (Hua et al, 1996). According to report by Li et al (1998), these organochlorine pesticides were mainly used in southeastern areas along the coast.

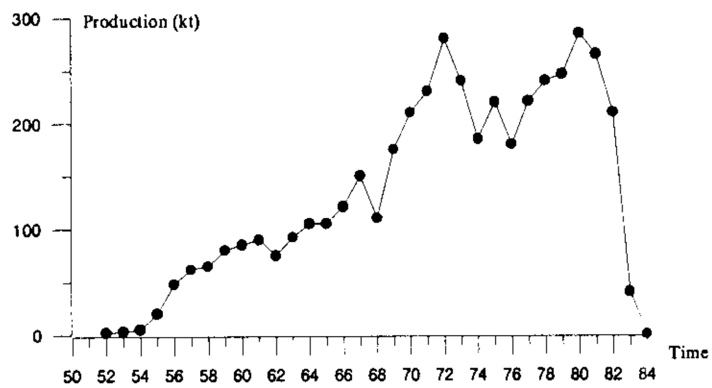

Fig. 1. Annual technical HCH production in China during beginning in 1952 to banned in 1984

Table 1 lists BHC and DDT concentration in soil and sediment in different stage in China.

The data in Table 1 show that the high residues of organochlorine pesticides both in terrestrial soils and sediments from the Changjiang estuary were seriously polluted by DDT and BHC before prohibiting to use DDT and BHC, and decreased largely after prohibiting to use DDT and BHC. But the residue of DDT and BHC in soils was still higher than that in sediments in any stage. Because the pesticides in sediments come from soil, the marine environment problem in Changjiang Estuary about DDT and BHC still depend on partly decreasing of pesticides residue in soil.

Table 1. The concentration of DDT and BHC in different material before and after prohibiting to use DDT and BHC in China (ng/g dry wt)

China		before DDT	before BHC		after DDT	after BHC		now DDT	now BHC	
Changjiang River	soil	246	740	1981 (1)	154	109	1985 (4)	10	12	1994(6)
Xianjiang River	Sediment		314	1983 (2)						
Changjiang Esuary	Sediment	6.9~ 16.0	0.95~ 5.9	1981 (3)	0.56~ 1.85		1992 (5)	0.22~ 0.31	0.35~ 0.47	1997(7)

(1)Huang, 1989(2)Wang,1984 (3)Lin,1983 (4)Zhou, 1986 (5)Ye, 1995 (6) Lin, 1995 (7) This paper

The dilution of organochlorine pesticides by bedload also present in core. The vertical distribution of BHC and DDT in core Meso and C1 present in Fig 2. According to dating by Pb-210, core Meso and C1 consist of new sediments in recently ten years, this is, these sediments are accumulated after prohibiting to use DDT and BHC. The BHC and DDT content in core Meso range 0.158~0.449ng/g and 0.176~0. 940ng/g respectively in the past 13 years, and in core C1 range 0.105~0.360ng/g and 0.039~0.220ng/g respectively in the past 10 years. The results show that the concentration of DDT and BHC has decreased to lower level. The content in Meso is little higher than that in C1, the reason be different between sediment character of two cores. The core Meso contains little sand content, which belong to clay sediment, but the core C1 contains high sand content as silt-sand sediment. Obviously, the core Meso has higher organic matter content (higher loss of ignition (LOI)), and higher DDT and BHC content. Cu distribution in cores proves also this character. This is resulting of clay sediment has finer particle, more surface area and charges so that it has higher absorption capacity. There is much evidence to indicate that organic matter is the predominant factor controlling the capacity of sediment to bind organochlorine compounds (Karickhoff, 1984; Di Toro et al., 1991). This would result in preferential organochlorine accumulation in sediment layer with a high organic content. In the two cores, the BHC and DDT contents have some relative large change. The reason may be diversity effect of transport and dilution of bedload, re-suspension of sediments and bio-disturb of benthic animal year by year. For example, the mass flux from the Changjiang River to sea would vary largely in some years due to large flood and soil erosion caused by global climate change and insufficient vegetation protection. This phenomena exist also in long core in which sediment contain higher organochlorine pesticides content as described in below.

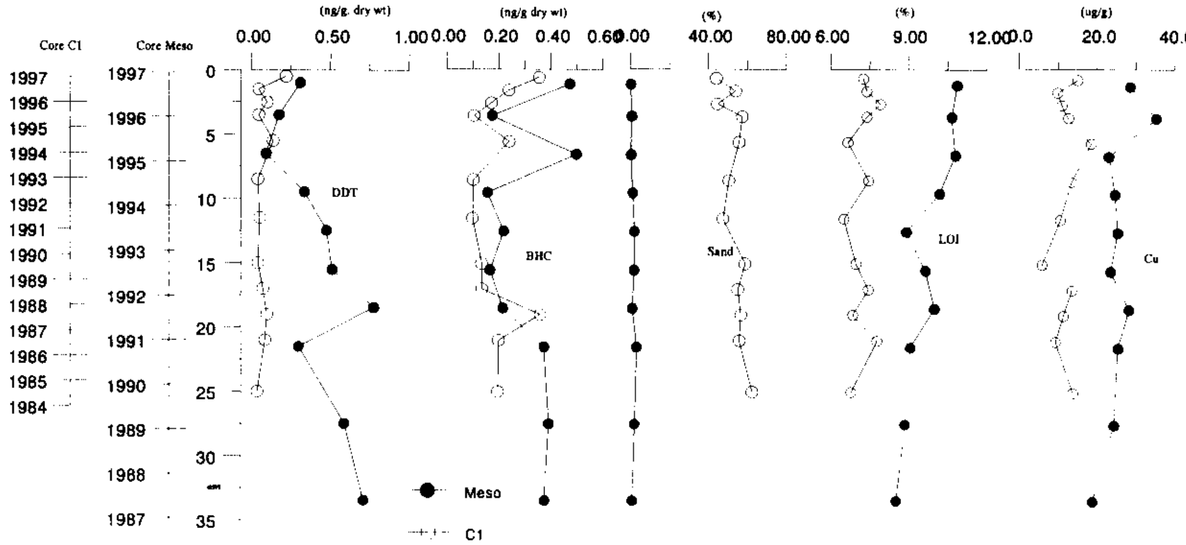

Fig. 2 The distribution of DDT and BHC and other parameters in short cores

In addition, the composition of BHC isomers in core shows Fig 4. The composition for each BHC isomers in core were relative stable, α-BHC and β-BHC were two dominant form about 35% for each in core. But the composition of BHC isomers in sediment had been changed compared to BHC production. In China, the BHC production contained 65-70%α-BHC, 5-6%β-BHC, 13% γ-BHC, and 6%δ-BHC (Cai, 1992). The composition of α-BHC in sediment increased and β-BHC decreased compared to BHC production. It was result of high volatilization of α-BHC and high absorption of β-BHC. In particular, β-BHC is easy enriched into organisms.the composition of BHC isomers in sediment was similar to soil, it represents also that BHC in sediment come mainly from soil.

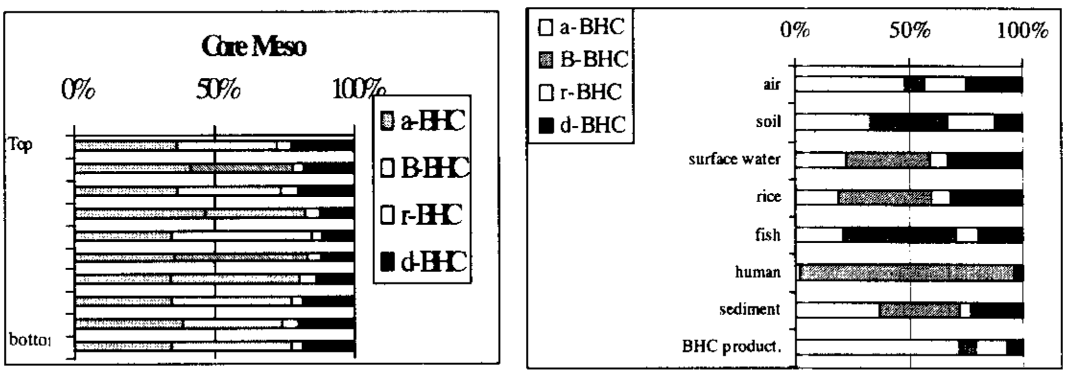

Fig. 4 The composition distribution of BHC in sediment core and in air, soil, water etc. in China

3.3.2 Vertical distribution of BHC and DDT in core sediment from the Changjiang estuary

Fig 5 shows the sand content, water content and organochlorine pesticides contents in the long core B1. B1 station is near to north mouth of the Changjiang River to East Sea. Because Pb-210 analysis of core B1 can't be finished yet, it is difficult understanding exactly its sedimentation rate and origin. Basing on previous research materials, the sediment of B1 originate mainly from the Changjiang River, but there is some possibility that suspension sediment of Yellow River may be transported by Yellow Sea Coastal Current (Chen, 1989). The distribution of sand content in core B1shows that sand content is relative stable, except for some individual year. Sediment of core B1 should be silt sediment,.

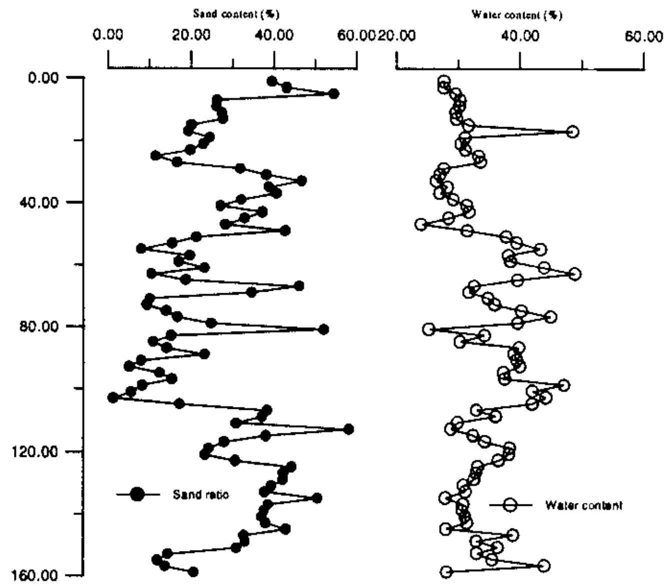

Fig. 5 The vertical changes of BHC and DDT contents in cores B1 from Changjiang estuary

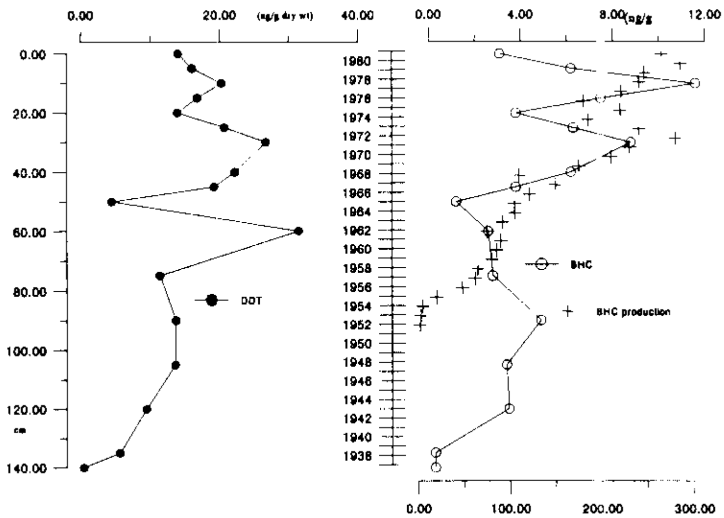

Fig.6 The vertical changes of BHC and DDT contents in cores G8410 from Changjiang estuary

To study completely marine organic pollution history of the Changjiang estuary, we investigated the organochlorinated pesticides pollution history in core B1 sediment in the Changjiang estuary by 210Pb dated method. The analysis results show in Fig 5 (the measurement is going on and not finished). Meantime, we combine another core analysis results (Lin, 1983) of

G8140 which locates on same survey area in the Changjiang estuary (location shows in Fig 1).

Fig. 6 shows the vertical changes of BHC and DDT contents in cores G8410 from Changjiang estuary. Because of lack of detail annual production of DDT, we can't compare between DDT content in core with production. But basic trend of production of DDT is similar to BHC. If we take the organochlorine pesticides usage as a pollution event, BHC distribution in core reflect well the whole process of this event. This distribution also presents that the sedimentary rate of G8410 was stable. According to this rate, the DDT high peak in core should occur about 1972, there was little difference with the high peak of DDT usage in 1976 (Hua, 1996)

Compared to core Meso and C1, the content of DDT and BHC was higher one to two order magnitude. Lower contents of organochlorine pesticides in core Meso and C1 indicates that this event was past in sediment record. However, the contents in suspended material is also high (Ye, 1995), it will still has some effect on marine environment.

From the distribution in cores, there is an obvious character that effect of DDT and BHC on marine environment of Changjiang Estuary is rapid process. This is, when large amount of DDT and BHC was used, Changjiang Estuary received rapidly a large amount of organochlorine pollutants from Changjiang River drainage as final sink place, and persevere it for a long time due to its persistence. Therefore these pollutants as pollution resource would polluted seriously marine ecosystem. But in another hand, with stop using these pesticides, a large amount bedload from upper Changjiang River will dilute the content of DDT and BHC, and put it into deeper sediment. It cause that the content of DDT and BHC in surface sediments decrease rapidly to lower level, therefore this process decrease the impact on marine environment of Changjiang Estuary. Although these persistence substance exchange also still to overlay water by bio-turbulence and molecular diffusion.

3.3.3 Accumulation rate into the sediment

Using the organochlorine pesticides concentration in the sediment core (Cs; pg/g dry wt) from the Changjiang, its annual accumulation rates into the sediments can be estimated. The following equation was employed for estimating the rate (F; pg/cm3.y):

$$F=\eta \times Rs \times d \times Cs$$

Where

Rs ------ the sedimentation rate (cm/y)

d ------ the sediment core density (g/cm3 wet wt)

η------ the sediment water content (%)

The Rs was defined as 2 cm/y as described above. The d was estimated from the average wet weight of sediment layers in unit volume and found to be 1.2 g/cm3 wet wt. Water content in the core sediments is assumed to be a constant 35%.

The estimated organochlorine pesticides accumulation rates into the new sediments after prohibiting to use DDT and BHC are presented in Fig 7. Unfortunately, it was quite difficult to understand variation of organochlorine pesticides accumulation rates in different cores, because of the lack of comparable data so far reported. The present DDT and BHC accumulation rate in this study was about 0.35~0.8 ng/cm2.y and 0.55~1.2ng/cm2.y for surface sediment. It is interesting that this sedimentary accumulation rate is similar to atmosphere input to water in Alaska (Iwata, 1993). Although Armstrong et al (1987) and Iwata et al (1993) pointed out that only a small frction of organochlorine transported with suspension particle from water into sediment.

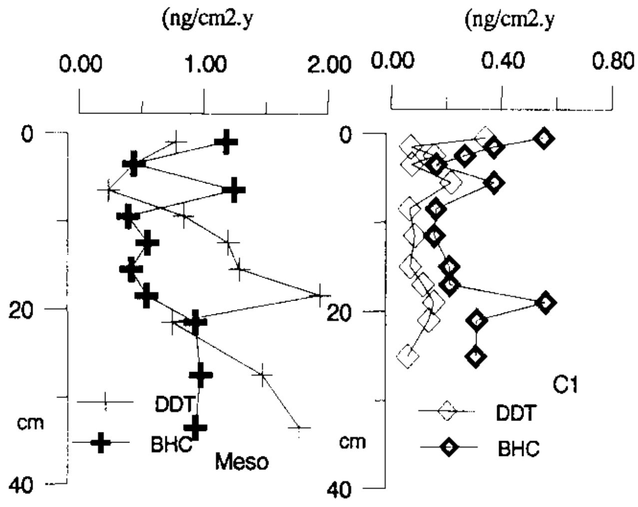

Fig 7. The estimated organochlorine pesticides accumulation rates into the sediments

3.4 Conclusion

The content distribution of DDT and BHC in surface sediments of different time and cores can represent the organochlorine pesticides pollution record and trend. The results show that most serious pollution stage about DDT and BHC has past. The content of DDT and BHC in the newest sediments have decreased to lower level about 0.25~0.31ng/g and 0.35~0.47ng/g respectively. DDT and BHC content also relate to sediment constitution, which in clay sediment is higher than other sediment. Due to persistence of DDT and BHC, its distribution in core obviously relate to its production and reflect the pollution record. The distribution in core shows also that DDT and BHC pollution on the Changjiang Estuary is relative rapid process, due to dilution by large bedload from Changjiang River and high sedimentary rate.

Reference

Sheng Yin, 1997, Marine environment pollution and environment protection, *Environment Science Development*, 5(1):67-75, (in Chinese)

Albone, E.S., Eglinton, G., Evans, N.C., 1972. Fate of DDT in Severn Estuary sediments. Environ. Sci. Technol. 6, 914-919.

Latimer J. S, Quinn J G, 1996, Historical trends and current inputs of hydrophobic organic compounds in an urban estuary: the sedimentary record, *Environ. Sci. Technol.* 30: 623-633

Chang Jianfang, Zhou Huaiyang, Zheng Haisheng, 1998, the stratiographal records of environment pollution history after industrialization, *Donghai Oceanography*, 16(3): 64-69, (in Chinese)

Lin Minji, Lin Zhifeng, Zheng Wenqing, et al, 1983, Determination of recent sedimentation rate and sedimentation of the East China Sea Continental Shelf by BHC dating, In: *Proceedings of international symposium on sedimentation on the continental shelf, with special reference to the East China sea*, China Ocean Press, 868-878pp

Lin Minji, Lin Zhifeng, Zheng Wenqing, 1986, On modern of the East China Sea Continental Shelf by BHC dating, *Taiwan Strait*, 5(2): 132-138, (in Chinese)

Ye Xinrong, Yang Hefu, Zhuo Jianfeng, 1991, On the PCBs, BHC and DDT in water of the Changjiang Estuary and adjacent coastal areas, *Marine Environment Science*, 10(4):52-56, (in Chinese)

Ye Xinlong, Lu Bing, 1995, The distribution of organic pollutants in the Changjiang Estuary and adjacent coastal areas, *Donghai Oceanography*, 13(3-4):72-83, (in Chinese)

Hua Xiaomei, Shuang Zhengjun, 1996, The production and use of pesticides in China and factor analysis of environment pollution, *Environment Science Development*, 4(2):33-45, (in Chinese)

Bignert, A; Olsson, M; Persson W., et al; 1998, Temporal trends of organochlorines in Northern Europe, 1967-1995. Relation to global fractionation, leakage from sediments and international measures, Environmental Pollution, 99(2):177-198

Karickhoff, S.W. , 1984. Organic pollutant sorption in aquatic systems. J. Hydraul. Engin. 110, 707-735

Di Toro, D.M., Zarba, C.S., 1991, Technical basis for establishing sediment qulity criteria for nonionic organic chemicals using equilibrium partitioning. Environ. Toxicol. Chem. 10, 1541-1583.

Iwata, H; Tanabe, S; Sakai, N; et al, 1993, Distribution of persistent organochlorines in the oceanic air and surface seawater and the role of their global transport and fate, Environ. Sci. Technol. 27, 1080-1098.

Iwata, H; Tanabe, S; Sakai, N; et al, 1994, Geographical distribution of persistent organochlorines in air, water and sediments from Asia and Oceania, and their implications for global redistribution from lower latitudes, Environmental Pollution, 85(1):15-33

Baker, J. E., Eadie,B.J. & Eisenreich, S.J. (1991). Sediment trap fluxes and benthic recycling of organic carbon, polycyclic aromatic hydrocarbons and polychlorobiphenyl congeners in Lake Superior. Environ. Sci. Technol. 25, 500-509.

Preston, M. R. (1988) in : Riley, J.P.(e.d.) Marine Pollution. Chemical Oceanography, Vol.9. Academic Press, London, pp.55-196.

Everarrts, J.M., Heester,R., Fischer, C.V. and Hillebrand,M.T.J.(1993) Baseline levels of cyclic pesticides and PCBs in benthic invertebrates from the continental slope of the Banc d'Arguin(Mauritania). Marine Pollut. Bull., 26,515-521

WHO,(1979) DDT and its Derivatives. Environmental Health Criteria 9. World Healthh Organization, Geneva.

WHO,(1989) DDt and its Derivatives. --- Environmental Aspects. Environmental Health Criteria 83. World Healthh Organization, Geneva.

Li, Y.F., Cai, D.J. Singh,A. 1998, Thecnical Hexachlorocyclohexane use trends in China and their impact on the environment, Arch. Environ. Contam. Toxicol. 35, 688-697.